

Available online at [www.sciencedirect.com](http://www.sciencedirect.com)

**jmr&t**  
Journal of Materials Research and Technology  
journal homepage: [www.elsevier.com/locate/jmrt](http://www.elsevier.com/locate/jmrt)



## Review Article

# Overview of magnesium-ceramic composites: mechanical, corrosion and biological properties



F. Khorashadizade <sup>a</sup>, S. Abazari <sup>b</sup>, M. Rajabi <sup>a</sup>, H.R. Bakhsheshi-Rad <sup>c,\*</sup>,  
Ahmad Fauzi Ismail <sup>d</sup>, Safian Sharif <sup>e</sup>, Seeram Ramakrishna <sup>f</sup>, F. Berto <sup>g,\*\*</sup>

<sup>a</sup> Department of Materials and Metallurgical Engineering, Iran University of Science and Technology, Tehran, Iran

<sup>b</sup> Department on Materials and Metallurgical Engineering, Amirkabir University on Technology (Tehran Polytechnic), Tehran, Iran

<sup>c</sup> Advanced Materials Research Center, Department of Materials Engineering, Najafabad Branch, Islamic Azad University, Najafabad, Iran

<sup>d</sup> Advanced Membrane Technology Research Center (AMTEC), Universiti Teknologi Malaysia, 81310, Johor Bahru, Johor, Malaysia

<sup>e</sup> Faculty of Engineering, Universiti Teknologi Malaysia, 81310, Johor Bahru, Johor, Malaysia

<sup>f</sup> Nanoscience and Nanotechnology Initiative, National University of Singapore, Singapore, 1157, Singapore

<sup>g</sup> Department of Mechanical and Industrial Engineering, Norwegian University of Science and Technology, 7491, Trondheim, Norway

## ARTICLE INFO

## Article history:

Received 14 July 2021

Accepted 30 October 2021

Available online 6 November 2021

## Keywords:

Mg-ceramic composites

Fabrication process

In vitro corrosion behavior

Biocompatibility

Biomedical applications

## ABSTRACT

Magnesium (Mg) and its alloys are potential metals for biodegradable implants because of several benefits, including a reduction of stress shielding effect in the implant for orthopedic application and the elimination of the step of a second surgery to remove the implant. On the other hand, unexpected degradation can cause the Mg to collapse, and the implant fails; thus, many studies have been done to control the rate of degradation of Mg alloys. Heterogeneous corrosion of these implants leads to rapid mechanical properties loss, limiting the clinical applications. Adding ceramic reinforcements to the Mg matrix as so-called Mg nanocomposites is one method to enhance the ductility and also mechanical properties of the Mg alloys without a noticeable weight cost. Good corrosion resistance and noticeable mechanical properties of the Mg-based nanocomposites have developed their applications. However, it is difficult to uniformly disperse the ceramic-based nanoparticles as reinforcements in the Mg matrix and attain desired characteristics. As a result, selecting Mg-ceramic composite production methods and reinforcing types to overcome Mg restriction and increase the favorable material features based on their applications is critical. As a result, this review study focus on the different fabrication techniques and reinforcement material types and their influence on Mg-ceramic composites' mechanical characteristics, in vitro corrosion performance and biocompatibility. The potential applications, and future research ideas of Mg matrix nanocomposite are investigated. The existing successes in this field are discussed, and future

\* Corresponding author.

\*\* Corresponding author.

E-mail addresses: [rezabakhsheshi@gmail.com](mailto:rezabakhsheshi@gmail.com) (H.R. Bakhsheshi-Rad), [filippo.berito@ntnu.no](mailto:filippo.berito@ntnu.no) (F. Berto).<https://doi.org/10.1016/j.jmrt.2021.10.141>2238-7854/© 2021 The Author(s). Published by Elsevier B.V. This is an open access article under the CC BY-NC-ND license (<http://creativecommons.org/licenses/by-nc-nd/4.0/>).

investigation areas are identified in order to boost the usage of degradable Mg-based composites.

© 2021 The Author(s). Published by Elsevier B.V. This is an open access article under the CC BY-NC-ND license (<http://creativecommons.org/licenses/by-nc-nd/4.0/>).

## 1. Introduction

Many people nowadays suffer from bone defects as a result of natural diseases or accidental accidents, rendering bone implants a major clinical procedure [1]. Internal fixation medical devices are needed for about one-third of all broken bones reported each year [2]. Artificial bone implants produced of biomaterials have recently been developed as a useful way of dealing with bone defects [3–5]. Artificial bone implants are mostly used to replace and repair damaged bones in order to return them to their natural physiological functions [3,6,7]. In the last five decades, biotechnology made many radical changes in the development of novel biomaterials that are primarily developed as implants to help, substitute, or improve the function of a body organ [8,9]. Biomaterials have been commonly utilized as medical implants (e.g. stent, bone graft, and heart valve), dental caring (e.g. implant and tissue), biosensor, bioelectrode, skin substitute, and drug delivery sets [10–12]. These materials must have good mechanical and physical properties, as well as being nontoxic, bio-functional, bio-adhesive, osteoconductive, corrosion resistant and wear resistant [12,13]. These properties are found in a variety of materials, which can be categorized into four major categories [14,15] including metals [16], polymers [17,18], ceramics [19,20], and composite materials [21,22]. Because of the better strength, fracture toughness and fatigue resistance of metallic biomaterial implants are favored for load-bearing applications over polymer-based or ceramic-based bioimplants [2,23]. 316L stainless steel (SS), cobalt-chromium (Co–Cr) alloys, commercially pure titanium (Cp–Ti), and Ti–6Al–4V are biocompatible and used as artificial organs in fracture surgical. The challenge with these metals is that they are not biodegradable; thus, in many of these cases, the second surgery is performed to remove the implants from the body after the recovery [24,25]. The development of biodegradable and biocompatible materials has revolutionized ceramics, polymers, metals, and biocomposite materials applications in healthcare applications [8,9].

Mg is a solitary macromineral found in the human body. Actually, 320–420 mg of Mg minerals are required by the human body each day [25]. Because of Mg's natural degradability, excellent biocompatibility, and high specific strength, it is a useful material in engineering applications and is often used as an important biomaterial [26,27]. Mg has one of the best biocompatibilities with human biology and the mechanical integrity with bone tissue, among other metal alloys [28]. So, Mg-based composites are widely used in transportation, aerospace, and especially the medical industry [29]. However, the high degradation rate of pure Mg with excessive H<sub>2</sub> gas releasing at the surrounding site of the implant limits the wide range of applications for Mg-based alloys [30,31]. In this regard, it was reported [25–28] that the high degradation rate of Mg alloys led to a loss of mechanical strength prior to

the completion of bone healing, which is also indicated as another major impediment to its possible applications. In clinical applications, composites development is a reliable solution to improve the corrosion and mechanical behavior of Mg. Biodegradable Mg-based composites with different compounds have been studied and showed significant achievements. Suitable choice of the reinforcement can improve the Mg's resistance of the degradation and its mechanical behavior without reducing the biocompatibility of these composites [30]. For example, the reinforcements in these composites are calcium phosphate-based ceramics, calcium polyphosphate (CPP) [32,33], hydroxyapatite (HAp) [34–37], and tricalcium phosphate (TCP) [38,39]. Bio-ceramics classify into bio-inert, bioactive, and bioabsorbable materials. Even in the human body, bio-inert ceramic compounds retain their mechanical and physical characteristics. One of the most important benefits of bio-inert ceramics is their low chemical interaction, which makes them completely inert and biocompatible. When bioactive ceramics come into contact with fluids of the body, a chemical reaction occurs that causes the formation of newly created bone. These ceramics have good hardness and wear-resistant [40]. Yang et al. [41] demonstrated that reinforcement materials with high bioactivity operate as an apatite nucleus and cause an apatite deposition. The deposited layer on the Mg alloy surface is composed of Mg(OH)<sub>2</sub>, apatite, and another Mg-substituted apatite. This layer has the ability to fill corrosion pits and affect the rate of degradation in the human body. Ca–P compounds and partial Mg(OH)<sub>2</sub> precipitate on the surface of a Mg-based composite with a bioactive glass (ZK30/10BG) improved the composite's corrosion resistance [42]. In this perspective, another study depicted that Ca–P compounds could operate as a barrier to the diffusion of corrosive solution [43]. In this context, various fabrication procedures are utilized to produce degradable Mg-based composites for biological purposes. These routes are divided into two main methods: (1) powder metallurgy processing and (2) casting procedure. Powder metallurgy is a conventional and affordable method to produce Mg-based composites resulting in uniform reinforcement distribution in the Mg matrix. Powder metallurgy is made up of three steps: the blending of powder, preparation of green compact, and sintering [23]. Casting is the most common and cheapest procedure for producing Mg alloys and Mg-based composites. In this method, first, this metal is heated to more than 750 °C in an inert atmosphere furnace to prevent oxidation, then pouring the melt into the mold and allowing it to solidify. The condition of the procedure has a significant impact on the microstructure, biocompatible and mechanical properties [40]. Zhou et al. [44] exhibited that numerous investigations have been conducted in recent decades regarding the wide range of Mg-based biomaterials for biomedical applications, including Mg/Mg alloys and bioceramics [2,7], bioglasses [8,9] reinforcements, and

polymers [10,25]. Many researchers [25,44,45] have made significant contributions to the advancement of production methods. The purpose of this review paper is to outline the most recent significant breakthroughs in the Mg-based composites encapsulated with ceramic reinforcements and the progress of their processing methods. Moreover, the biocompatibility and degradation behavior of Mg matrix composites for orthopedic applications are also discussed. Also, the main challenges and problems in the promising study on Mg-based materials for biomedical applications are stated.

## 2. Use of Mg in biological devices: historical overview

Mg has a long history of research as a biodegradable material. Mg was first used in biomedical applications by physicians in the late 1800s. Until the mid-twentieth century, experimental research proceeded with varying degrees of success [42]. The use of Mg bone fixation devices in medical applications goes back to the early 20th century, as evidenced by the case reports shown in Fig. 1 [41]. Edward C. House used Mg as a wire ligature to avoid bloodshed during surgery in many humans in 1878 [42,43]. Seelig was considering Mg for ligatures in 1924 and He used the results of Payr, Chlumsky, Lespinasse, and Andrews's research [46]. Gotthard Gossrau of I.G. Farbenindustrie AG developed an Mg rope in 1935 that was made up of a mesh of thin wires (less than 0.1 mm) wrapped around a thicker inner wire bundle or intertwined wire bundle [47]. McBride in 1938 and Maier in 1940 also conducted additional research on Mg as an implant, including compatibility and corrosion problems [48]. In 1917, Andrews first suggested the easily absorbed metal clips as a ligature and deep suture substitute [49], and later in 1986, Richard Jorgensen obtained a patent for an innovative haemostatic clip layout [50]. The study on the application of Mg metal in biomedical proceeded on a small scale all across the twentieth century and the new phase of Mg research has been began in the early 2000s [51]. In the current research, Mg metal has been used to improve bone strength and interfacial potency as orthopedic implants [52].

Mg metals can be found in a variety of orthopedic surgery fascination instruments, such as screws, and plates. Mg alloy can give appropriate support to the bone during the healing process and eventually degrades [25,53]. For cardiovascular applications, Conformité Européenne (CE)-approved biodegradable Mg-based vascular closure device, called “Velox CD”, has been produced through transluminal technologies [53]. Mg-based materials also have other applications (e.g., coronary scaffolds and ureteral stents) in medical [54]. For the treatment of esophageal cancer, Wang et al. [55] have utilized an Mg alloy (Mg–Zn–Y–Nd) stent. The Mg alloys have prevented the growth of esophageal cancer cells and had a better biodegradability and lower hardness than 317 L stainless steel. Wu et al. [56] have investigated the possibility of biodegradable Mg alloys to be used in tracheal stents.

## 3. Requirement for Mg composite development

Mg is an important nutrient for human survival and the fourth most plentiful element in the human body [25]. Previously, pure Mg has been used to create degradable metallic biomaterials [23]. Recently, the biomaterial society has paid close attention to the production of Mg-based alloys with improved corrosion resistance and mechanical properties for biomedical applications [23]. Many studies have shown that producing Mg alloys with controllable degradation rates is in high demand. To satisfy this demand, the development of new composites based on Mg alloys in conjunction may be a good option [57,58]. Because of the toxicity of many alloying components, researchers have developed the idea of special bioactive particle reinforced Mg-based metal matrix composites (MMCs) as degradable metallic biomaterials for medical application [59,60]. The incorporation of particles as reinforcements into the Mg matrix has been shown to enhance mechanical properties [61,62]. The composites' increased strength can be due to the influences of the following points: (i) Orowan mechanism: The presence of dispersed small-sized particles in the matrix inhibits dislocation penetration,

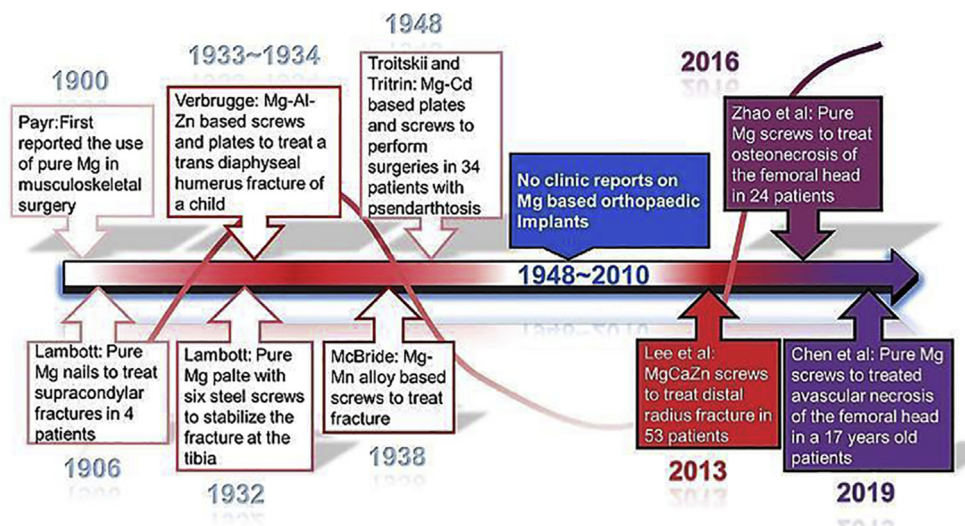


Fig. 1 – Typical human case reports on Mg bone fixation devices since the early 20th century [41].

resulting in dislocation bowing. Usually, when the particle density in the material is low, dislocation bowing is more probable to appear. (ii) Due to the strong interfacial bonding between the matrix and the particles, the material has adequate load-bearing ability. (iii) Internal thermal stresses are made as a result of the big variation in thermal expansion coefficients between the matrix and the particles, (iv) The work hardening mechanism is caused by a mismatch between reinforcement particles and the matrix. (v) When the particles have a wide surface region, more dislocations are formed. Furthermore, a high density of the particles leads to dislocation accumulation [63,64]. In addition, as compared to other metallic-based composites, Mg composites had superior biocompatibility, so it is a good choice for biomedical applications. Mg is the fourth most common mineral in the human body, and it is so vital for the formation of bone and soft tissue in the human body [25]. A normal adult needs 21–28 gr of Mg to maintain his activities. The introduced daily allowance of Mg is 250–350 mg for an adult [41,65–68]. It is worth noting that extra Mg ions will be carried by the blood vessels and quickly eliminated by the urinary system; thus, it does not harm the body. Figure 2 depicts the process of selecting materials, manufacturing them into semi-products, designing and developing devices, and producing the device to its final performance as an implant, as well as a variety of common biomedical applications for designed biodegradable Mg alloys [24,41]. Orthopedic fixation systems, such as bone screws, bone pins, and bone plates, are used to fix during bone healing, stent, and some devices for final medical devices [41,69].

#### 4. Commonly used reinforcement materials: ceramic reinforcement

The composite reinforcements are used to improve the properties of the composites according to their application. In other words, the selection of reinforcement is so critical in the composite [13,25,41,70], and the important issue in producing degradable MMCs for medical applications is the selection of biocompatible, biodegradable, and nontoxic particles as a reinforcement [23,35,58,71–73]. Mg composites are being used to improve mechanical properties and the rate of degradation in the biological environment. Incorporation of bioactive ceramic particles to Mg-based improve corrosion properties,

bioactivity, and tissue interactions is a great way to use composite biomaterials to provide innovative characteristics for medical purposes [9,13,31]. A category of materials with properties similar to the mineral sections of bone appears to be useful for hard tissue [58,63]. Mg composites have been produced using a variety of reinforcement materials to use in the medical applications. The main ceramic reinforcements of Mg-based composites such as titanium dioxide ( $\text{TiO}_2$ ), zirconium oxide ( $\text{ZrO}_2$ ), hydroxyapatite (HAp), beta-tricalcium phosphate ( $\beta$ -TCP), calcium polyphosphate (CPP), fluorapatite (FAP), bioactive glass (BG), bredigite (Bre), zinc oxide (ZnO), and magnesium oxide (MgO) have been reviewed in the following sections.

##### 4.1. Hydroxyapatite and Mg/HAp composites

HAp is a calcium phosphate mineral, and its chemical composition is  $\text{Ca}_5(\text{PO}_4)_3(\text{OH})$  [74]. The good bioactivity of HAp allows it to make a direct chemical bond with bone that makes it useful [57]. In a physiological environment, HAp has excellent bioactivity and biocompatibility. Furthermore, it has a low level of solubility. When compared to natural bone, its toughness and compressive yield strength are both higher [25,36]. As compared to other types of reinforcement, HAp has been widely used in Mg implant-bone. A lot of studies have shown that adding HAp into the Mg matrix can improve biocompatibility, corrosion, and the mechanical resistance [23,34,35,75]. Jaiswal et al. [76] evaluated mechanical, corrosion, and biological performance of the Mg–3Zn/HAp composite. Figure 3 shows FESEM images of immersed samples for different periods [76]. The images clearly show that HAp content aids in the formation of apatite layers. It is also affected by the duration of immersion. With increasing immersion time, more apatite layer was observed. The formation of apatite layers on 5 wt% HAp composite was higher (Fig. 3), which explains why the degradation rate of 5 wt% HAp composite was lower than bare Mg. Detachment of the apatite layer due to the high corrosion rate can be seen on the surface of the 10 wt% HAp composite after 28 and 56 days of immersion [76]. In comparison to other phosphate groups, the HAp has a special function of biocompatibility. In comparison to  $\beta$ -TCP, hydroxyapatite particles have very poor solubility in human body fluid [74,75].

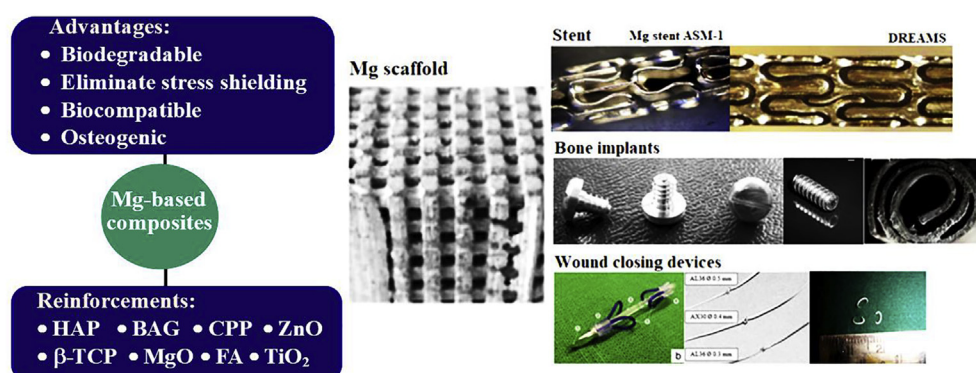
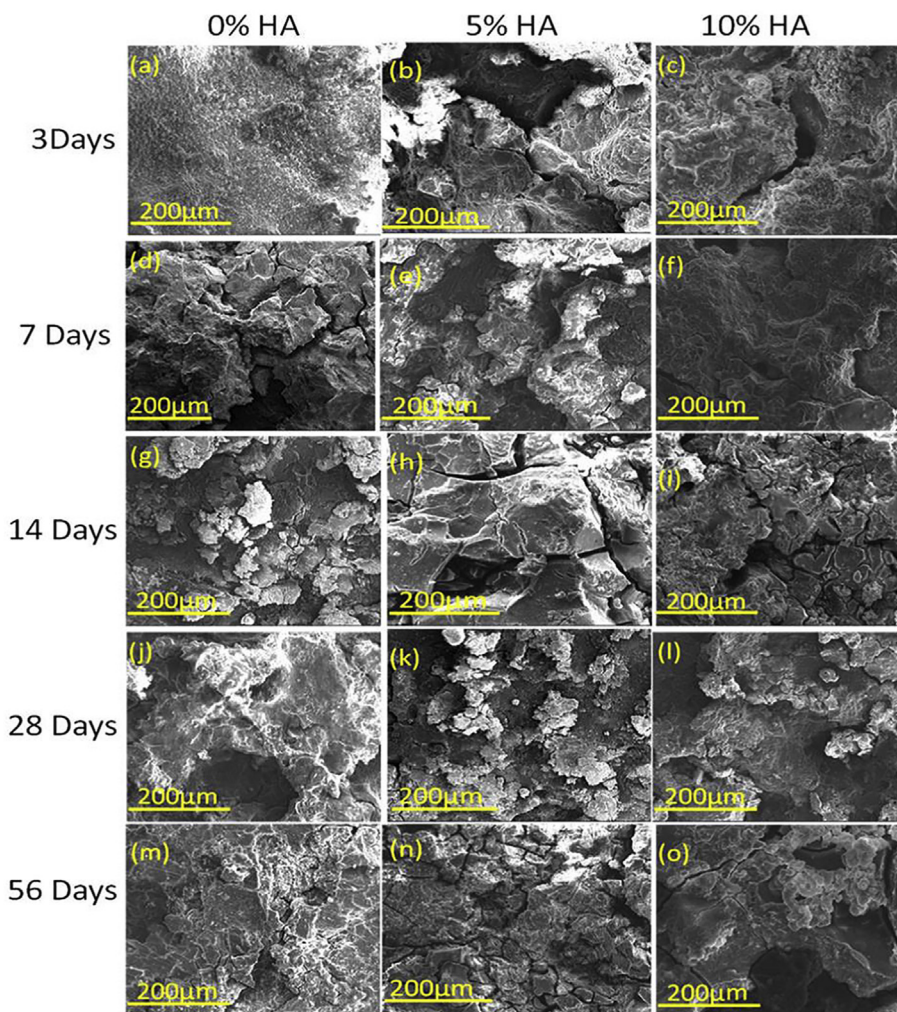


Fig. 2 – Reinforcement types, advantages and biomedical applications of biodegradable Mg alloys [24,41].



**Fig. 3 – SEM micrograph of Mg–3Zn/xHAp composite structures immersed for (a, b, c) 3 days (d, e, f) 7 days (g, h, i) 14 days (j, k, l) 28 days and (m, n, o) 56 days [76].**

Nakahata et al. [77] employed a spark plasma sintering technique to prepare Mg/HAp composites with varying compositions and grain sizes. Their findings demonstrated that the presence of HAp increased both mechanical characteristics and corrosion resistance. The findings also revealed that a finer grain size improved the majority of the qualities required in material for an orthopedic implant. According to Khalil et al. [78] the decrease in relative density and microhardness of nanocomposites with increasing HAp content can be due to clustering of HAp nanoparticles or too low sintering temperature, which for pure HAp reaches approximately 1000 °C. They discovered that composites containing Mg/1 to 3 wt.% HAp had the best mechanical characteristics. Mechanical characteristics of a Mg/HAp/MgO nanocomposite for biomedical applications were investigated by Khalajabadi et al. [79]. Their results showed that the UTS of the composite decreased due to the addition of MgO and the reduction of HAp from 27.5 to 5 wt. %; nevertheless, the compressive failure strain dramatically improved, which could be attributed to a decrease in HAp particle

agglomeration. In this regard, Razavi et al. [59] reported that grain boundary ledges formed by the agglomeration of multiple glide planes under applied compressive stress acted as obstacles to the movement of dislocations, resulting in pile-ups and thus an increase in the samples' ultimate compressive strength and a decrease in their compressive failure strain. Furthermore, the presence of hard HAp particles along the matrix particle surfaces may reduce matrix particle deformation induced by dislocation movement and twinning. Nevertheless, the interfacial bonding between the matrix and the filler particles, as well as the content of reinforcement, influences the efficiency of constraining particle deformation. Even though a greater amount of HAp as reinforcement may increase the material's strength, the compressive failure strain may degrade due to HAp particle agglomeration. Microvoids can also be created between the matrix and the agglomerates of the HAp particles, which may propagate cracks during mechanical testing and, as a result, reduce the compressive failure strain of the specimen [63].

#### 4.2. $\beta$ -tricalcium phosphate and Mg/ $\beta$ -TCP composites

Another calcium phosphate used in the body is  $\beta$ -TCP with the chemical formula  $\text{Ca}_3(\text{PO}_4)_2$  [58]. The orthopedic industry has paid much attention to  $\beta$ -TCP since Albee and Morrison reported it in 1920 for bone tissue [80]. The  $\beta$ -TCP is bioresorbable in biological environments in comparison to HAp, and it has osteoinductive properties. Its crystallographic structure and chemical formula, which are similar to bone mineral components, result in the preferred biological characteristics [57]. Despite the fact that Mg and  $\beta$ -TCP are quickly dissolved, Mg/ $\beta$ -TCP composites demonstrated a desirable rate of degradation [58]. Wang et al. [38] reported that the Mg–Zn–Zr/ $\beta$ -TCP composite had better corrosion behavior than the Mg–Zn–Mn alloy. On the surface of the composite, the corrosion products had been favorable compounds for bone growth [38]. The mechanical behavior of Mg–Zn–Zr/ $\beta$ -TCP composite was investigated by Zheng et al. [81]. Because of the low wettability between Mg–Zn–Zr and reinforcements, they have improved  $\beta$ -TCP with MgO to disperse the  $\beta$ -TCP in the Mg crystal core properly to prevent agglomeration of nanoparticles [82]. He et al. [39] have reported that Mg–3Zn–0.8Zr composites reinforced by  $\beta$ -TCP composites have a better ultimate tensile strength than Mg–Zn–Zr matrix. Because of more dislocation accumulation and the fine grain size. The incorporation of  $\beta$ -TCP to matrix improves corrosion resistance, which may be due to the microstructure modification [39]. Cui et al. [32] investigated the mechanical characteristics of  $\beta$ -TCP reinforced ZK61 Mg alloy composite via spark plasma sintering. The average Vickers values of ZK61/ $\beta$ -TCP composite shift from 74.02 to 94.81 HV<sub>0.1</sub>, and the hardness value increases as the  $\beta$ -TCP content increases as shown in Fig. 4a [32]. The results revealed that by adding  $\beta$ -TCP to the ZK61 alloy matrix, the hardness of the matrix could be enhanced since the presence of harder  $\beta$ -TCP particles in the matrix would have stronger limitations on the matrix's local deformation. As indicated in Fig. 4b [32], the compressive strength of the ZK61 sample is  $271 \pm 6$  MPa, while composites containing 5 wt%, and 15 wt%  $\beta$ -TCP have higher compressive strengths of  $338 \pm 13$ , and

$402 \pm 9$  MPa, respectively. This is because the use of  $\beta$ -TCP as reinforcements reduces the grain size of the matrix in the composite, and fine grain hinders dislocation movement [32].

#### 4.3. Bioactive glass (BG) and Mg/BG composites

Bioactive materials such as fluorapatite, HAp, and BG are primarily studied as reinforcements because of their inherent osteogenic properties. BG has a significant advantage over these reinforcements in terms of solubility and biocompatible degradation products [83]. Hench [84] suggested BG as a bioactive and biodegradable material for medical use in the human body in 1970. BG is a ceramic with a silicate base that consists of phosphorus pentoxide ( $\text{P}_2\text{O}_5$ ), sodium oxide ( $\text{Na}_2\text{O}$ ), silicon dioxide ( $\text{SiO}_2$ ), and calcium oxide ( $\text{CaO}$ ) [84]. Huan et al. [83]. Utilized extrusion to produce a ZK30-BG composite and have reported that adding BG to ZK30 matrix improved corrosion resistance in comparison to ZK30 alloys [83]. In another study, Dutta et al. [85] fabricated Mg/BG composites by spark plasma sintering method. They have reported that BG particles have distributed uniformly. The authors also claimed this Mg-based composite with high modulus could be used as a bone fracture fixation layer [85]. Generally, according to the conclusions of many studies, the rate of degradation, bioactivity, and tensile strength of Mg implants can all be enhanced by using nano BG reinforcement [36,40]. Among the reinforcements, BG reinforcements have great benefit over other particles due to better solvability and biodegradable products [57,71,84–86]. Over the years, many changes to the original 45S5 BG have been applied to enhance the ability to biodegrade and bond with the bone. BG has the ability to form a favorable physical bonds with the bone, stimulating bone growth far away from the implant place [86,87]. Dutta et al. [88] demonstrated that 10wt.% BG addition increased the corrosion resistance of Mg-10BG composites when compared to pure Mg (Fig. 5i). The fluorescence images of MG-63 cells after 1 and 3 days of culture are shown in Fig. 5ii [88]. All of the composites had nearly identical cell attachments on day 1. For Mg-10BG samples, highly confluent live cells were observed on

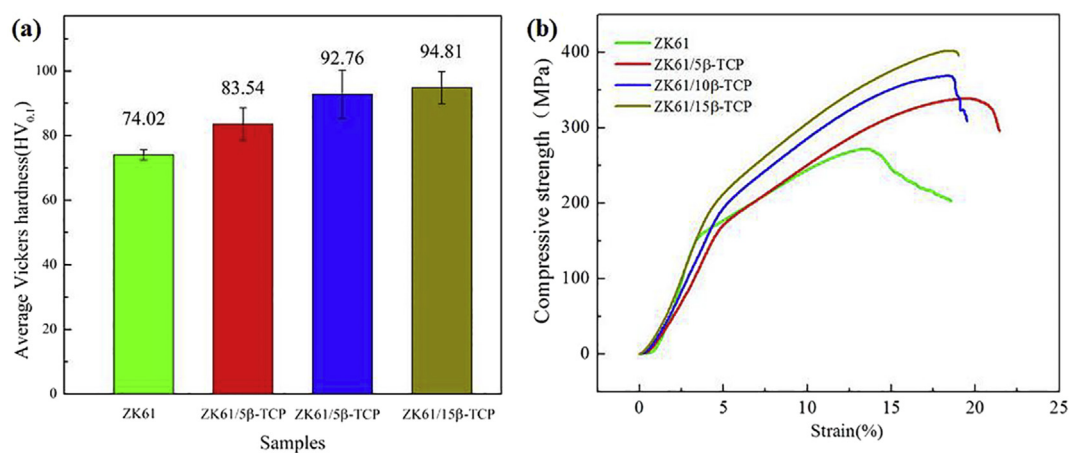


Fig. 4 – (a) Average hardness and (b) compressive stress–strain curves of ZK61 and ZK61/ $\beta$ -TCP composites [32].

day 3. For Mg-15BG samples, only a few dead cells (indicated by red) were found.

Yang et al. [89] used an enhanced sol–gel process to create mesoporous bioglass (MBG) with a high pore volume (0.59 cc/g) and a large specific surface area (110.78 m<sup>2</sup>/g), which they then incorporated into a Mg-based composite via laser additive manufacturing. The results showed that MBG caused in-situ apatite layer deposition, which significantly reduced the corrosion rate of the Mg matrix. Furthermore, the MBG as reinforcing particles were homogeneously dispersed inside the Mg matrix, limiting grain development during laser powder bed fusion. The mechanical properties of Mg-based composites were improved owing to the strengthening influence of nanoparticles and fine grain strengthening. Yin et al. [90] created ZK30/xBG composites with varying amounts of BG particles (5, 10, and 15 wt %) that were uniformly distributed in the ZK30 alloy matrix. The addition of BG particles increased the microhardness of the composites. Furthermore, they discovered that encapsulating BG in the ZK30 alloy improves the apatite production ability and corrosion resistance of the Mg-based matrix. Cell viability assays revealed that ZK30/10BG was more compatible than ZK30 without BG. In this aspect, ZK30 having 10% BG demonstrated greater bioactivity, cell viability, and a lower corrosion rate than other samples. In another study, Yang et al. [91] employed MBG as a carrier of copper (Cu) ions to produce Cu-doped MBG (Cu-MBG), which

was then inserted into a Mg-based scaffold constructed using laser additive manufacturing. Cu-MBG with high bioactivity successfully promoted in situ apatite deposition, which functioned as a protective layer and thereby decreased the degradation rate of the Mg matrix. Cu-MBG also increased cell response, including cell growth and adhesion. They presented a new technique based on these findings to simultaneously increase the biomedical Mg-based material's antifungal effect, degradation behavior, and cell response.

#### 4.4. Calcium polyphosphate (CPP) and Mg/CPP composites

Calcium polyphosphate (CPP) is an important inorganic component of the human body's hard tissues, such as bone and teeth [92,93]. CPP is a dense calcium phosphate with a calcium: phosphorus ratio of 1:2. It is composed of linear regular tetrahedral groups (PO<sub>4</sub>) [94]. Although calcium polyphosphate has low solubility in water, CPP is also sensitive to hydrolytic degradation due to phosphate group scission [95]. The product of degradation (calcium orthophosphate) is produced naturally, and it is capable of being metabolized. In vivo investigations have revealed that porous calcium polyphosphate promotes fast growth of bone and can be degraded at a specific rate in vivo by selecting the favorable particle size at the beginning [25,33,96]. Feng et al. [33] investigated the

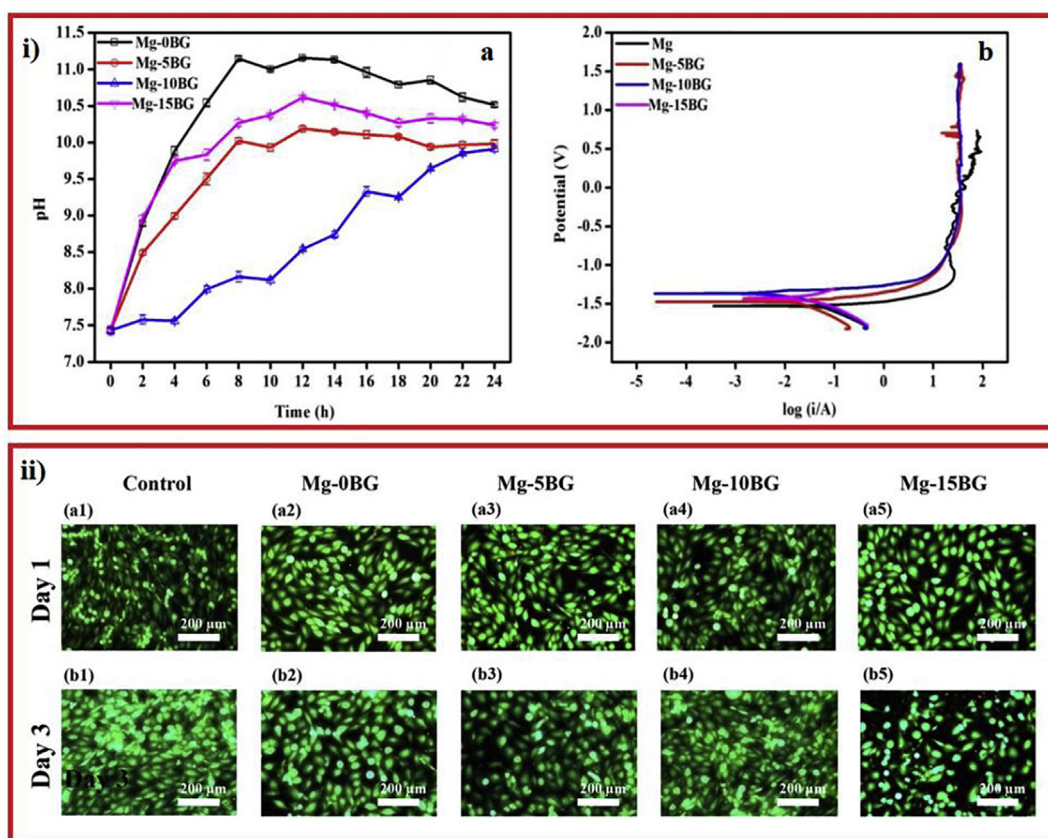


Fig. 5 – (i) Variation of the solution pH as a function of time for Mg-BG composites immersed in PBS at 37 °C (a), and potentiodynamic polarization curves (Tafel Plot) of Mg-BG composites (b), and (ii) Fluorescent images of live (green) and dead (red) MG-63 cells after day 1 (a1–a5) and day 3 (b1–b5) [88].

mechanical properties and degradation behavior of Mg/CPP composites in vitro and have concluded that composite strength increased as the grain became finer by addition CPP [33]. In addition, other studies have shown that the Mg/CPP composite is steady in vivo conditions and does not disintegrate in humid or dry air at temperatures up to 1200 °C [25,33,96]. ZK60A/CPP composites have good mechanical properties and controllable degradation rates, according to Feng et al. [33], and thus have the potential to be used as load-bearing bone implants. SEM images of the tensile fracture surfaces of ZK60A alloy and composites with 5 and 10 wt.% CPP are shown in Fig. 6 [33]. On the fracture surfaces of all the specimens, there are numerous ductile dimples. It is worth noting that the 10 wt.% CPP-containing composite also has interfacial detachment between CPP and matrix, which results in large pores on the fracture surface [33].

#### 4.5. Fluoroapatite (FA) and Mg/FA composites

Fluoroapatite (FA) is also known as calcium fluorophosphate.  $\text{Ca}_5(\text{PO}_4)_3\text{F}$  is the formula for this phosphate mineral [63]. In comparison with HAp, fluoroapatite has a lower rate of dissolution and higher cell adherence [93,97] that greatly boosts phosphate activity, resulting in increased osteoconductivity [73,98,99]. FA particles facilitate forming bone-like apatite and mineralize and crystallize calcium phosphate by adjusting the amount of fluoride [23,99]. So, FA has the potential to be a viable candidate for the production of Mg-based composite [23]. Razavi et al. [73] developed an Mg/FA composite using a blending–pressing–sintering process, and after 72 h of immersion in SBF, a bone-like apatite layer was formed on the surface of the AZ91-20wt.% FA nanocomposite. According to the results of the study, adding FA

reinforcement into the Mg matrix could enhance mechanical properties, decrease the rate of corrosion and facilitate the formation of the apatite layer on the surface providing more protection of the AZ91 alloy. These bone-like apatite precipitations can prevent corrosion and improve the composite's biocompatibility and bioactivity that is so important for medical applications [73].

#### 4.6. Zinc oxide (ZnO) and Mg/ZnO composites

ZnO reinforcement is widely used in biomedical applications like biomedicine and bioimaging. According to recent research, nano-ZnO can facilitate osteoblast proliferation and bone development, as well as has significant antimicrobial activity [100,101]. Lei et al. [102] produced the Mg–ZnO nanocomposite via in situ powder metallurgy method. The results of this study showed that as compared to pure Mg, adding ZnO to the pure Mg matrix increases tensile strength and hardness. Adding 20 wt.% of the ZnO particles to the Mg matrix reduced the ductility of the Mg–ZnO composite by 1.43%. Furthermore, in comparison to pure Mg, the Mg-xZnO composites showed better corrosion resistance [102]. Selvam et al. [103] investigated the dry sliding wear test of the Mg-based composite reinforced with ZnO particles. They have reported that the wear rate of these composites was increased by increasing the load and sliding velocity [103]. According to Tun et al. [104] the improved ultimate tensile strength in Mg/ZnO composites can be due to the strengthening effect of ZnO particles in the Mg matrix. The authors have stated that the reason for the increased, ultimate compressive strength in Mg/ZnO composites is the difficulty in twinning and slip-dominated flow as a result of grain refinement [104].

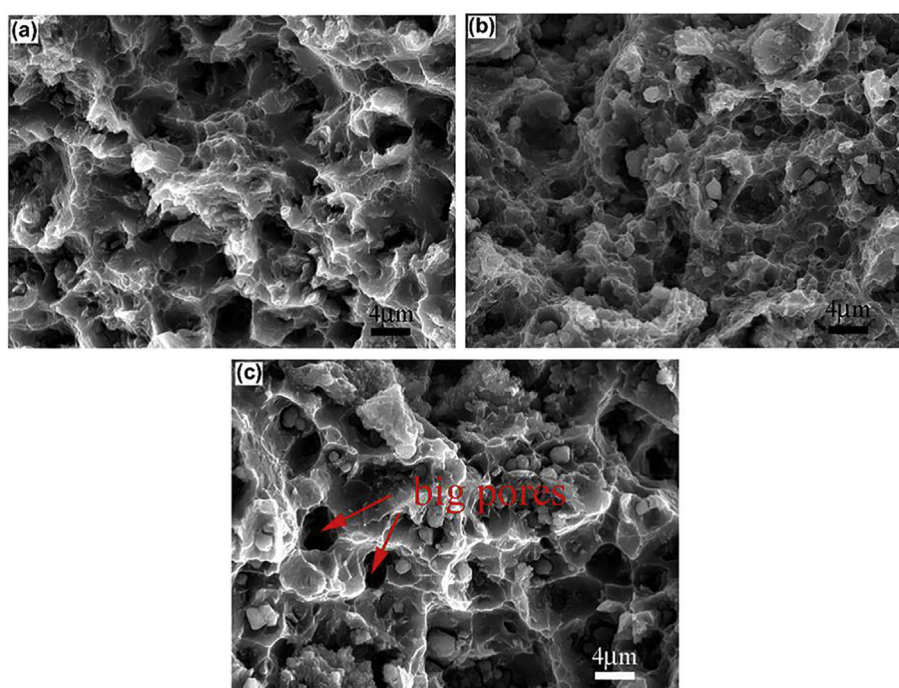


Fig. 6 – SEM micrographs of the tensile fracture surfaces of (a) ZK60A alloy, (b) 5 and (c) 10 wt.% CPP-containing composites [33].



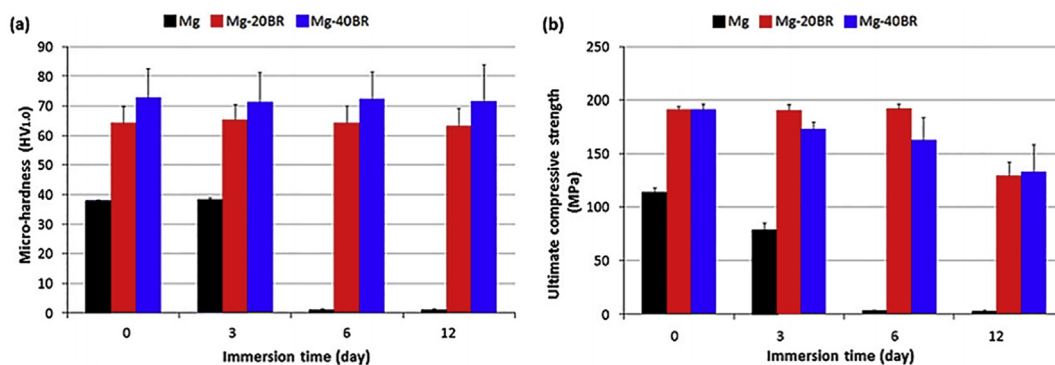


Fig. 7 – Ultimate compressive strength (a) and micro-hardness (b) of the composites as a function of immersion time in DMEM [70].

#### 4.7. Bredigite (Bre) and mg/Bre composites

Bredigite ( $\text{Ca}_7\text{MgSi}_4\text{O}_{16}$ ) is a  $\text{CaO-SiO}_2\text{-MgO}$  bioceramic with high biocompatibility and cytocompatibility [105,106]. In physiological solution, Bre can form HAp, which is the main component of the bone [106]. Many studies have shown that Bre can be used as a reinforcement material in medical applications. Wu et al. [107] stated that they used Bre in an Mg matrix to improve its biocompatibility and mechanical properties, making it appropriate for load bearing application [107]. Dezfuli et al. [70] produced the Mg-Bre composite with the presence of 20 vol% Bre reinforcements in the Mg matrix showed 67% higher ultimate compressive strength and 111% improved ductility. In vitro degradation rate of this composite was reported 24 times less than pure Mg. Consequently, due to the reported properties of the Mg-Bre composite even after 288 h of immersion in the culture medium is suitable for use in medical applications [70]. For bone implant applications, Dezfuli et al. [70] investigated Mg-matrix composites containing various amounts of Bre. Their findings revealed that adding bredigite to Mg improved the composite's degradation behavior, bioactivity, and biocompatibility. According to their findings, there were no significant differences in micro-hardness values before and after immersion in DMEM as shown in Fig. 7a [70]. The mechanical behavior of the composites in DMEM was affected by degradation, causing the UCS to gradually decrease from 190 to 130 MPa over the duration of 12 days as presented in Fig. 7b [70].

#### 4.8. Magnesium oxide (MgO) and Mg/MgO composites

MgO is biodegradable in vivo, and  $\text{Mg}(\text{OH})_2$  is its degradation product. MgO also has antibacterial properties as well as good thermal, and mechanical properties [108]. Several studies have shown that the presence of MgO particles in the Mg composite improves its mechanical and biological properties. For example, Goh et al. [109] have produced an Mg/xMgO composite using the disintegrated melt deposition method. The results of mechanical tests showed that the addition of 1vol% nano-sized MgO enhanced the yield tensile strength, ultimate tensile strength and microhardness of the

Mg/xMgO composite. Lin et al. [110] stated in another study that the as-cast  $\text{Mg-3Zn-0.2Ca/xMgO}$  composite had finer grain than the matrix alloy. Furthermore, the interfacial bonding between MgO and  $\alpha\text{-Mg}$  seemed greatly effective [110]. The mechanical and degradation properties of AZ61-RGO/MgO composite are shown in Fig. 8 [111]. Shuai et al. [111] prepared AZ61-RGO/MgO composites by SLM method, and their result showed AZ61-RGO/MgO composite had higher compressive strength and hardness with 241.2 MPa and 108 HV, respectively, than AZ61-RGO composite (Fig. 8a). Furthermore, AZ61-RGO/MgO composite had a lower corrosion rate of 1.05 mm/y compared to the AZ61-RGO composite (1.32 mm/y) in a weight loss test (Fig. 8b). At the same time, the pH of the AZ61-RGO composite in SBF rose rapidly at first, and then slowed down after ~3 days. On the other hand, the pH variation of the AZ61-RGO/MgO composite in SBF was much slower throughout the immersion period (Fig. 8c). In comparison to the AZ61-RGO composite, the above findings showed that AZ61-RGO/MgO composite had better corrosion resistance. The potentiodynamic polarization curves of the AZ61-RGO/MgO composite showed a lower corrosion rate, which was further supported by the potentiodynamic polarization curves (Fig. 8d) [111].

#### 4.9. Titanium dioxide ( $\text{TiO}_2$ ) and Mg/ $\text{TiO}_2$ composites

$\text{TiO}_2$  has received a great deal of coverage in recent studies [64,72,112].  $\text{TiO}_2$  particles are usually utilized to enhance the bioactivity and corrosion resistance of the matrix. Aeroxide  $\text{TiO}_2$  P25 particles have a specific composition of 25% rutile and 75% anatase phase [64,112,113]. Since the pure Mg and  $\text{TiO}_2$  are both bio-inert and biocompatible, investigating the characteristics of the Mg/ $\text{TiO}_2$  composite is useful for biomedical applications [113,114]. Khosroshahi et al. [115] produced an AZ80-1 wt.%  $\text{TiO}_2$  nanocomposite. They have claimed as compared to AZ80 alloy, the addition of 1 wt. % nano  $\text{TiO}_2$  has caused a substantial reduction in grain size and an improvement in microhardness and ultimate tensile strength [115]. In another research, Meenashisundaram et al. [113] found that by adding  $\text{TiO}_2$  (2.5 vol.%) as a reinforcement, the fracture strain, proof stress and ultimate tensile strength

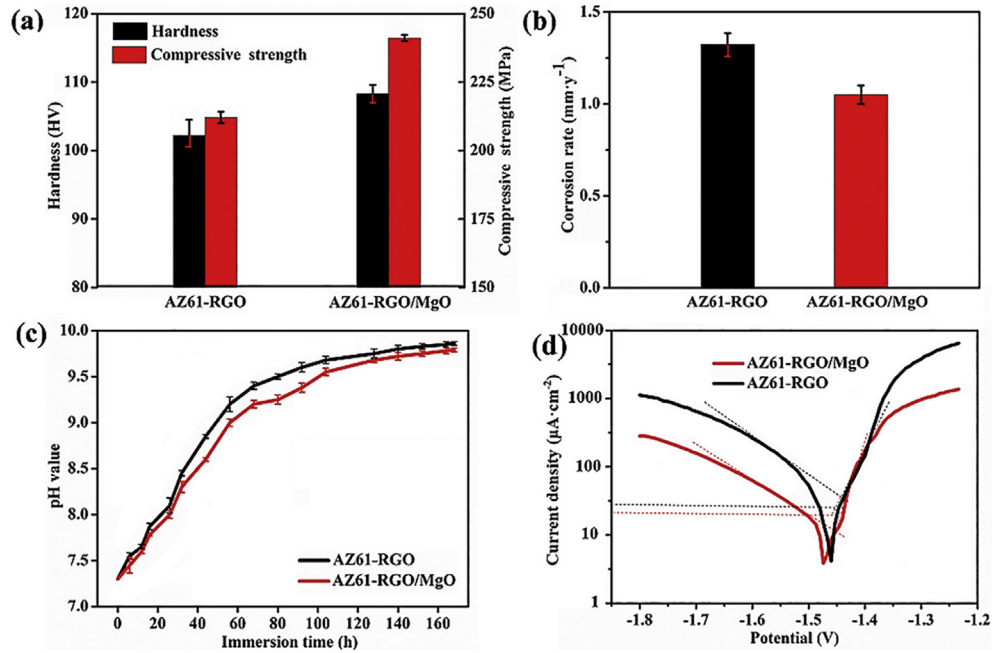


**Fig. 8 – The mechanical and degradation properties of AZ61-RGO/MgO and AZ61-RGO composites: (a) compressive strength and hardness, (b) corrosion rates and (c) pH variations measured by weight loss test, (d) polarization curves [111].**

of pure Mg enhanced by 31%, 37%, and 9%, respectively [113]. Bolokang et al. [72] fabricated Mg–Sn–TiO<sub>2</sub> composites for biomedical application. Figure 9a–9d shows SEM images of Mg, Mg–TiO<sub>2</sub>, and Mg–Sn–TiO<sub>2</sub> after nitridation at 650 °C [72]. The surface morphology of Mg powder after annealing in an O<sub>2</sub>/N<sub>2</sub> gas mixture is shown in Fig. 9a. The SEM surface

morphology proves a two-phase structure, with small cuboidal type particles and strides-type with steps pattern. The surface morphology of the unmilled-nitrided Mg–TiO<sub>2</sub> powder is shown in Fig. 9b. The agglomeration of particles is still visible after nitridation. Figure 9c shows a 30 h milled and nitrided Mg–TiO<sub>2</sub> powder at 650 °C. It is clear that the ball

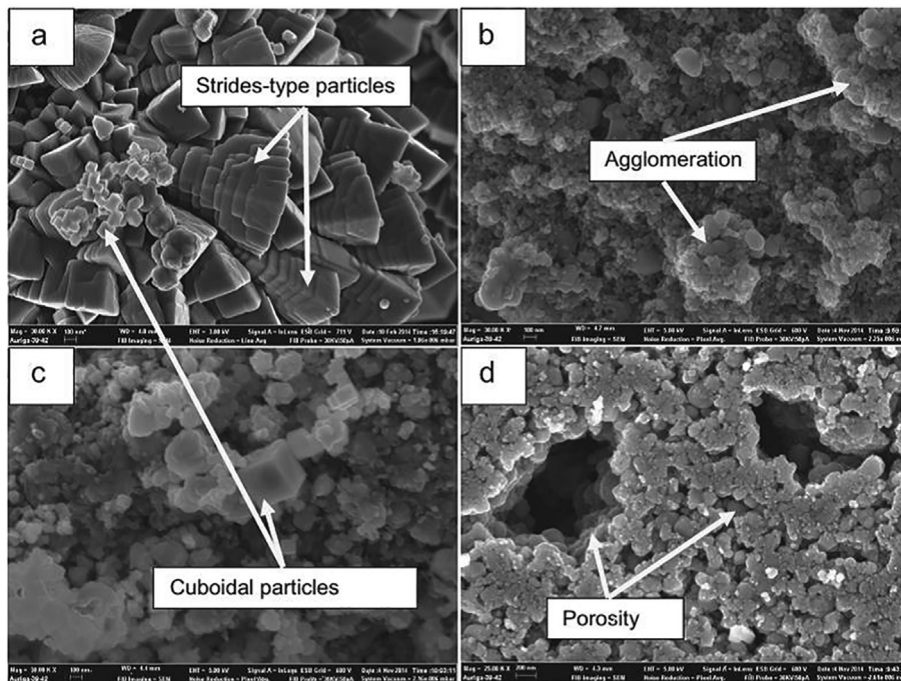


**Fig. 9 – SEM images of (a) MgON (b) unmilled and nitrided Mg TiO<sub>2</sub>, (c) 30 h-milled Mg–TiO<sub>2</sub> and (d) Mg–Sn–TiO<sub>2</sub> powders [72].**

milling and annealing have caused a phase transformation, as illustrated by the appearance of a new particle network. The particles appear to be interconnected, welded, and grouped into large and small pores, as shown in Fig. 9d. These pores are irregular in shape and range in size from ~200 nm (small pores) to about 800 nm (large pores) [72].

#### 4.10. Zirconium oxide (ZrO<sub>2</sub>) and Mg/ZrO<sub>2</sub> composites

In recent years, there has been an increase in the demand for the development of Mg-based composite materials with high specific mechanical characteristics. So far, many reinforcing particles, such as ZrO<sub>2</sub>, have been added to the Mg matrix to enhance the mechanical properties of the alloys [116]. ZrO<sub>2</sub> has high mechanical and fracture toughness, giving it a wide range of applications as a biomaterial. ZrO<sub>2</sub> has an advantage over other ceramics due to the transformation toughening property of its microstructure. The same property can be seen in the components made of ZrO<sub>2</sub> [44]. According to studies, adding ZrO<sub>2</sub> particles to a Mg matrix improves the mechanical characteristics and biocompatibility of the material [117,118]. For example, Navazani and Dehghani [117] introduced ZrO<sub>2</sub> particles to AZ31 Mg plates using FSP and discovered that the particles increase the grain refinement and improve the mechanical properties of composites. FSP was used by Vignesh et al. [118] to develop AZ91D- ZrO<sub>2</sub> surface composites. The combination of FSP and ZrO<sub>2</sub> was reported to reduce grain size, as well as break and disperse secondary particles. The dispersion of ZrO<sub>2</sub> particles can raise the accumulated surface potential, boosting composite corrosion resistance [116]. Hassan et al. [119] used a disintegrated melt deposition

approach followed by hot extrusion to strengthen Mg with nano-ZrO<sub>2</sub> particulates. Their findings demonstrated that the addition of nano-ZrO<sub>2</sub> particulates in the Mg matrix improved hardness, 0.2% YS, and UTS but decreased ductility. Another study used the blend press sinter hot extrusion approach to develop [120] nano-ZrO<sub>2</sub> particles containing Mg nanocomposites. The presence of nano-ZrO<sub>2</sub> particulates in the Mg matrix increased microhardness and 0.2% YS, with no change in UTS and a considerable increase in ductility and work of fracture. The increase in ductility of a Mg matrix as a result of grain refinement, the presence of sufficiently uniformly dispersed reinforcing particles, and slip on an extra non-basal slip system [121]. Rahmani et al. [122] used hot pressing to develop Mg–ZrO<sub>2</sub> nanocomposites, and their results show that increasing the volume fraction of ZrO<sub>2</sub> increases the composite's UCS compared to pure Mg. The hardness of the nanoparticles is assumed to be responsible for the improvement, as is a layer of MgO that surrounds the grains and operates as a reinforcement phase. Furthermore, some strengthening mechanisms, such as Orowan and thermal mismatch, cause the generation of dislocations, which leads to greater strength.

Friction stir processing (FSP) was employed to create AZ31/ZrO<sub>2</sub> nanocomposites by Qiao et al. [116]. The addition of ZrO<sub>2</sub> particles enhanced the microhardness and tensile strength of FSP-ZrO<sub>2</sub> composites. The composites' strengthening mechanisms are primarily grain refinement strengthening and Orowan strengthening. When compared to the base metal, the presence of ZrO<sub>2</sub> particles increases brittleness while decreasing elongation. Besides, grain refinement and the barrier effect of ZrO<sub>2</sub> improve Mg alloy corrosion resistance in

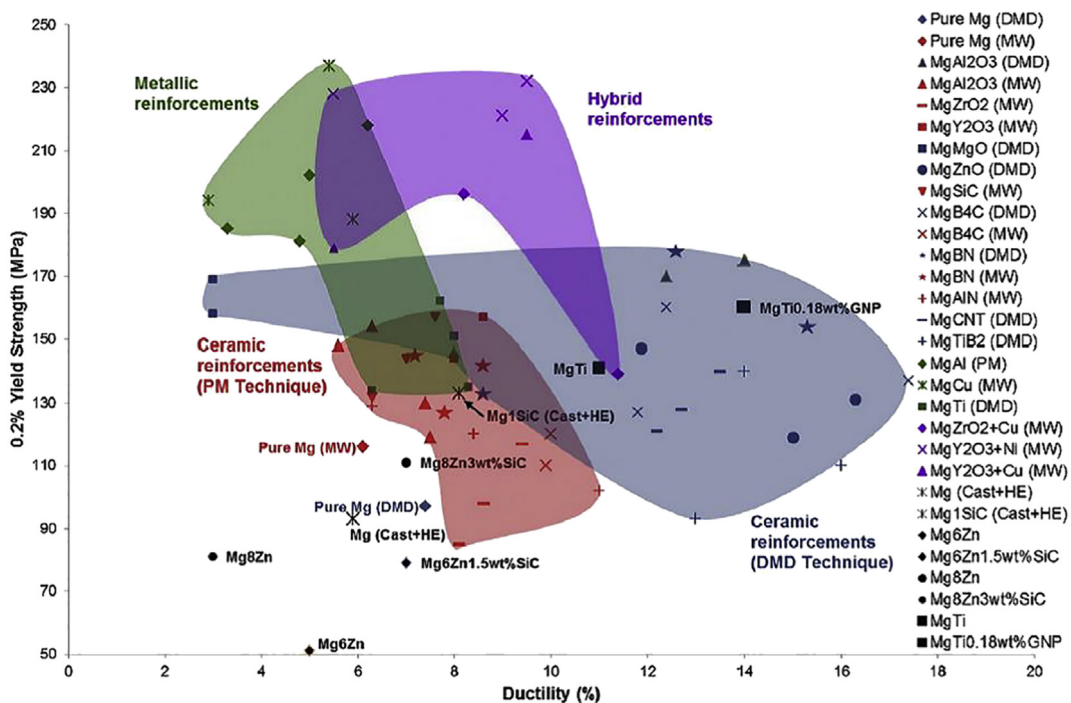


Fig. 10 – Bubble chart showing yield strength versus ductility for various types of Mg nanocomposites made using disintegrated melt deposition (DMD), microwave sintering (MW) assisted powder metallurgy (PM), and cast and hiped (Cast-HE) techniques [126].

simulated bodily fluid [116]. Rahmani et al. [123] produced Mg-based nanocomposites containing 1.5, 3, and 5 vol.% ZrO<sub>2</sub> nanoparticles by a hot compaction method. According to the findings, there is a linear relationship between tensile strength and reinforcement phase composition, and it is inversely proportional to reinforcement particle size. Mg composites boosted with 5 vol.% ZrO<sub>2</sub> nanoparticles had tensile strengths that were 2.5 times higher than unreinforced Mg. The presence of nano-size reinforcements [124,125] would improve the Mg matrix's ductility and mechanical properties, as seen in Fig. 10 [126]. Ceramic reinforcements enable the best results in terms of ductility. Grain refining (due to the pinning effect of reinforcements), crystallographic direction variation, and non-basal slip system activity are some of the important reasons that increase the ductility of the composites compared to the matrix (e.g., Mg and/or Mg alloys). Metallic reinforcements can improve mechanical properties such as yield strength because of proper wettability and appropriate bonding between matrix and nanoparticles [126]. Also, solid solution hardening improves the strength of metal matrix composites [124]. Adding nanoparticles to the Mg matrix led to an increase in the mechanical properties of the Mg-based nanocomposite. Its reasons are several mechanisms such as the Hall–Petch theory, Orowan strengthening, load transfer efficiency, strain hardening, locking of dislocations mechanism, and mismatch strain between the Mg and the nanoparticles [124,126].

## 5. Fabrication methods for Mg bone implants

There are a few popular manufacturing methods used to produce Mg-based composites. Powder metallurgy (PM), casting, wrought techniques, and laser additive manufacturing are the most commonly used methods, as described here. It must be noticed that the manufacturing method used can influence the applicability of Mg-based composites, and the manufacturing method has a direct effect on the microstructure and resultant properties, such as the degradation rate, mechanical properties, and biological behavior [9,41,127].

### 5.1. Powder metallurgy (PM)

One of the most common processing methods for producing composites is PM. The main benefit of this method is particle distribution uniformly in the matrix and a lower manufacturing temperature than the conventional casting method. In addition, PM is a low-cost method for producing Mg metal matrix composites (MMCs). Powder mixing, green compact preparing, and sintering are the three primary steps of the PM method [9,88]. One of the most serious issues is the agglomeration of the particles, which can be affected by particle size and manufacturing techniques. The limited wettability of ceramic nano-particles with the molten metal matrix is another main challenge in the manufacturing of metal matrix nanocomposites (MMnCs), which prevents the use of normal casting techniques for the production of MMnCs. But on the other hand, small powder aggregates are

prone to agglomeration, reducing their capacity to be homogeneously dispersed throughout the matrix for effective utilization of the strengthening potential. Furthermore, when the volume fraction of nanoparticles is high, dispersing them becomes much more challenging due to the increased possibility of colliding and creating clusters. As a result, uniformly dispersing a high volume proportion of nanoparticles in molten metal has never been accomplished or even assumed possible. PM is the most extensively used solid-state processing technology for producing MMnCs. Shahin et al. [128] exhibited that poor wettability of reinforcement, such as TCP, with the Mg matrix might result in uneven and quicker corrosion in the biological environment. Zheng et al. [81] modified the surfaces of  $\beta$ -TCP nanoparticles with MgO to obtain homogeneous dispersion in the Mg–Zn–Zr matrix. The mechanical characteristics of the composites were improved by uniformly dispersed  $\beta$ -TCP nanoparticles via a grain refinement strengthening mechanism. Several different potential techniques have been presented to address this issue. When the volume fraction of nanoparticles is high, dispersing them becomes significantly more challenging due to the increased possibility of colliding and creating clusters. As a result, uniformly dispersing a high volume fraction of nanoparticles in molten metal has never been realized or even considered feasible [1]. However, compared to casting techniques, PM appears to be an appropriate route to distribute particles in the metal matrix uniformly. The initial powder is pressed into the desired form under extreme pressure and then sintered in the controlled atmosphere furnaces. The chemical and physical proceedings like recrystallization, diffusion, fusion welding, dissolution and combination occur during the sintering step, resulting in sintering densification [33,41,57]. PM also facilitates alloy design flexibility for various elemental or main alloy powder to achieve improved mechanical properties. Essentially, studies have shown that PM is competitive with casting, forging, or machining methods [127]. PM method is one of the most appropriate methods for manufacturing high melting point materials because it is the most cost-effective and energy-efficient method [129]. PM is an appropriate method for incorporating various types and volume fractions of reinforcements [61]. Many researchers have published the specifications of Mg-based composites, e.g., hardness, yield tensile strength, ultimate tensile strength, compressive strength, density, wear resistance, impact and corrosion resistance, manufactured using the PM method for biomedical applications [27]. The following are some of these studies. Li et al. [130] announced that PM was used to successfully manufacture ZK60–0.05 wt% diamond [130]. Xiong et al. [26] used ball milling to mix Mg powder and HAp powder for 4 h. This mixture was compressed using a cylindrical die made of steel at a pressure of 50 MPa. They have stated that Mg/HAp composites were produced by microwave sintering process for 10 min and these composites have higher density and better mechanical and biological properties than pure Mg [26]. In another study, PM was used to fabricate monolithic Mg and Mg-based nanocomposites with 2.0 and 0.5 wt% of Y<sub>2</sub>O<sub>3</sub> reinforcement, and microstructural characterization showed a relative distribution of yttria

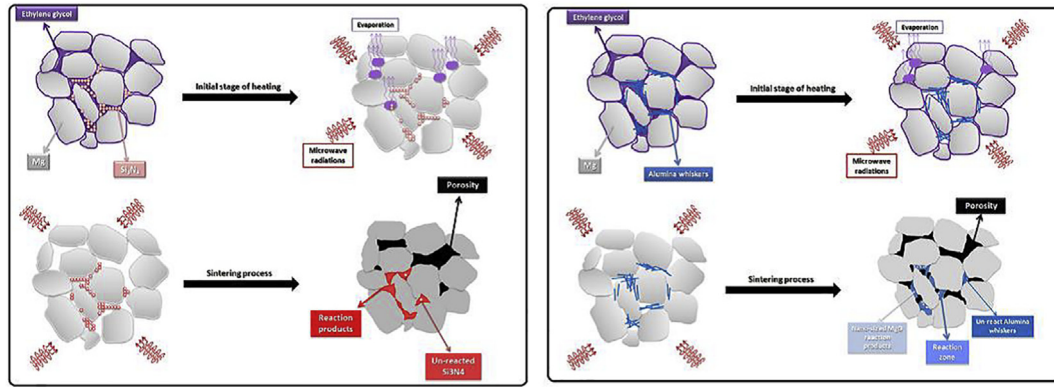
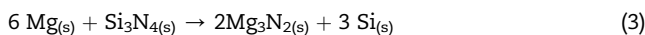
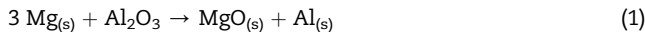


Fig. 11 – Schematic principle of porosities and reaction products formation during microwave sintering [132].

particles uniformly and the existence of nanopores. Tun et al. [131] reported that the composite containing 2.0 wt.% of  $Y_2O_3$  achieved the acceptable combination of mechanical properties by PM method [131]. Ghasali et al. [132] have created Mg/ $Al_2O_3$  and Mg/ $Si_3N_4$  MMC with a porosity of roughly 50% by microwave sintering technique at 650 °C. As shown in Fig. 11 [132]. The main steps during fast microwave heating are: 1) the initial heating stage is influenced by the type of the absorber particles, and ethylene glycol vaporization occurs, 2) the second stage heating process is in charge of forming bonds between Mg-particles densified at high temperatures. The interfacial interactions, which are accelerated by high local temperatures caused by high local heat sites, cause to proceed the reactions from (1) to (4) in the second stage [132].



## 5.2. Casting

Casting is the most common method to fabricate the composite. The matrix has been melted and particles are distributed in the matrix's molten state during the casting method. Mechanical or induction stirring is often used to facilitate the distribution of the reinforcements. That is why the stirring step is so important in this technique [9]. To produce special Mg-based composites, an appropriate casting method is required that provides uniform dispersion of reinforcements in the melted Mg, and using the ultrasonic vibration is helpful. Powerful impact coupling combined with local high temperatures has the potential to prevent agglomeration [61]. After adequate stirring, the molten material is poured into a pre-heated die of the desired form and begins to solidify [23]. The casting technique is the most widely used in the production of Mg-based implants since it facilitates the controlling of the alloy components [41]. Khanra et al. [75] manufactured

biodegradable Mg/HAp composites using extrusion after the casting method. Wang et al. [38] used suction casting to produce an Mg–Zn–Mn/C composite. This composite had a close-cell and compact structure. No cracks or holes were observed in the interface between the carbon scaffold and matrix. The results of mechanical tests revealed that the composite's ultimate compressive strength was higher than that of the original scaffold. Because Mg is so sensitive to oxygen, a neutral environment (such as Ar and SF6) is provided in the casting process [41]. Furthermore, in order to provide biomedical equipment, Mg bone implants must have special forms. Bone fixation systems typically need nail-shape structures and flat plates, while scaffolding of the bone requires the structure with pores. The casting process isn't appropriate to produce the final forms, but this method is useful for generating the basic material for subsequent procedures (such as wrought, extrusion, forging methods) [133]. However, the casting process is a suitable procedure for fabricating large volumes of Mg bone implants.

## 5.3. Wrought techniques

Due to the wrought Mg alloys' homogeneous microstructure and improved mechanical properties over as-cast alloys, wrought Mg alloys have attracted a lot of attention as lightweight structural materials. In the last decade, there has been significant progress in the field of wrought Mg alloys with suitable mechanical properties. Rolling, forging, and extrusion are some of the most popular wrought procedures used in the manufacture of Mg bone implants. Figure 12 shows all of these processing techniques [134–136]. Cao et al. [137] used hot rolling to develop a Mg-based alloy to homogenize the microstructure and reduce the secondary phase. Their result revealed that fine-grained hot-rolled samples possess uniform microstructure and fewer and smaller second phase particles, which reduces the corrosion rate. Khanra et al. [75] stated the existence of MgO in these composites is due to the reaction that occurs between Mg and HA in the melting step. Wu et al. [138] produced AZ91-SiCp composites using a step that combines extrusion and hot forging after stir casting. They have investigated the influences of these processes on the mechanical behavior and the microstructure and have reported that: a) the step

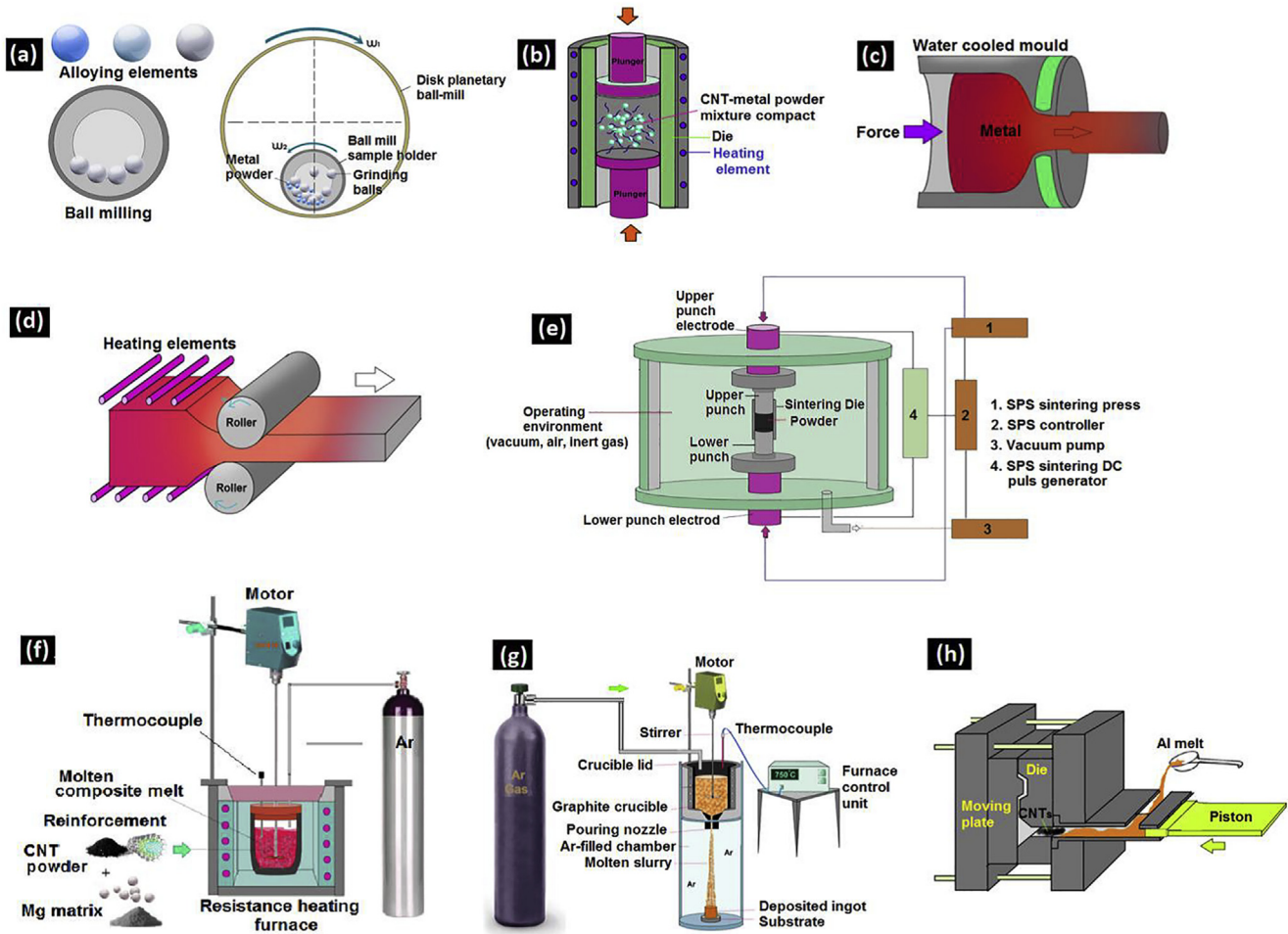


Fig. 12 – Different metallurgical methods for fabricating composites: (a) powder metallurgy [134,135], (b) hot press sintering, (c) hot-extrusion, (d) hot rolling, (e) spark-plasma sintering (SPS), (f) stir casting (SC), (g) disintegrated melt deposition (DMD) [135,136] and (h) high-pressure die casting [134,135].

combining extrusion and hot forging has been used for grain refinement in AZ91-SiCp composite, b) another advantage of using the step that combines extrusion and hot forging was the uniform distribution of reinforcements, c) the ultimate tensile strength and the yield strength of the AZ91 alloy reinforced by SiCp were significantly increased by using two-step processing, d) the plasticity of the AZ91-SiCp composite was enhanced using the extrusion method after forging step and e) the uniform distribution of the reinforcements and grain refinement led to an evident improvement in rate of work hardening in the extruded sample in comparison with the forged sample during tensile deformation at room temperature.

#### 5.4. Laser additive manufacturing

Nowadays, the digitization and analysis of patient data have significantly advanced over the last few years. Laser additive manufacturing (LAM) is an important method of the advances in additive manufacturing (AM) technology. This method enables the layer-by-layer fabrication of prosthetics and implants with specific anatomic surface shapes made of

a wide range of biocompatible or load bearing materials. Due to the digital process chain, it is possible to use specific and custom-made designs to handle the medical requirements [139]. Typically, the LAM process consists of the following [41]: 1) the data of the 3D model be prepared by computer; on the cylinder, 2) a layer of metal powder is sprayed, 3) the laser beam is adjusted by computer to scan the powder layer carefully and obtain a single layer, 4) the cylinder's height is reduced by one layer, and the roller created a new layer. Then the next layer is constructed on top of the previous layer till the requested design is produced. As previously stated, LAM is a modern production method that facilitates the direct production of desired products for small batches with specific structures or complicated shapes, and has recently been used for medical production [140,141]. It has been claimed that the thin matrix–reinforcement interface fabricated via laser processing methods can modify interfacial bonding and stress transfer. This causes various distortion mechanisms between matrix and particles to be modified during mechanical loading [142]. In medical science, the primary purpose of the process chain is the fabrication of personalized prosthetics and implants to fulfill the patient's needs [143].

The primary efforts to analyze the reactive material via the LAM method were made by melting the pure Mg [140,144]. Several papers [140–145] referring to the LAM process for Mg-based bone scaffold applications have been published recently. Li et al. [146] used the LAM method to produce interconnected porous Mg scaffolds based on the unit cell of diamond. This Mg scaffolds demonstrated appropriate mechanical supports and suitable degradation rates after one month in simulated body fluid. In comparison to other biomaterials, such as iron or titanium, Mg's melting point is so close to its boiling point, so Mg is rapidly oxidized, making a significant challenge for the laser forming process. However, among the AM technologies, selective laser melting (SLM) has been preferred to fabricate biodegradable Mg-matrix composites in a lot of studies. It seems that SLM is a successful method for producing biodegradable Mg-matrix composites [147–150]. Table 1 shows the manufacturing methods and properties of several Mg-based composites in comparison to their matrix by addition the various reinforcements. The information about the mechanical

properties of the Mg based composites is summarized in Table 2. Li et al. [146] fabricated biodegradable porous Mg by SLM. Figure 13a depicts the surface morphology, microstructure, and composition of WE43 scaffolds [146]. The surface of the samples on the circumference became relatively smooth after chemical polishing, but the roughness of the struts in the center remained high. On the surface of the as-polished specimens, flake-shaped, homogeneously distributed white second-phase particles were discovered (Fig. 13a). The stacking of melt pools in the build direction can be seen in all struts (Fig. 13b). In the as-built specimens, two distinct microstructural features: rose-like grains and cellular morphology were observed [146].

## 6. Strengthening mechanism of composite

The direct strengthening process in particulate reinforced MMCs is a development of the traditional composite strengthening processes. Load is transferred from the matrix

**Table 1 – Production methods and mechanical and corrosion properties of magnesium-ceramic composites.**

Author	Matrix	Reinforcement	Production method	Changing Properties in comparison to the matrix by addition the reinforcements
Meenashisundarama et al. [113]	Pure Mg	TiO <sub>2</sub>	Synthesized using disintegrated melt deposition technique followed by hot extrusion	Mechanical properties increased
Cui et al. [32]	ZK61	β-TCP	Spark plasma sintering	Hardness, compressive strength and corrosion resistance increased
Razavi et al. [73]	AZ91	Fluorapatite	Blending–pressing–sintering	Mechanical properties increased, the corrosion rate decreased
Feng et al. [33]	ZK60	CPP	Powder metallurgy	The ultimate strength and yield strength decreased and the corrosion resistance increased
Dutta et al. [88]	Pure Mg	Bioglass	Hot press sintering	Corrosion resistance and cytocompatibility increased
Kumar et al. [151]	AZ31	Al <sub>2</sub> O <sub>3</sub>	Innovative disintegrated melt deposition (DMD) process followed by hot extrusion	The corrosion resistance and in vitro biocompatibility improved
Cao et al. [152]	Pure Mg	ZnO	Spark plasma sintering	The corrosion rate decreased
Khanra et al. [75]	Pure Mg	HAP	Melting and extrusion route	Compressive strength increased, tensile strength decreased
Xiong et al. [26]	Pure Mg	HAP	Microwave sintering method	Mechanical and biological properties enhanced
Ghasali et al. [29]	Pure Mg	B <sub>4</sub> C	Powder metallurgy route (Comparison between microwave and spark plasma sintering)	Bending strength and microhardness improved (bending strength and microhardness of SPS samples rather than microwave samples)
Campo et al. [35]	Pure Mg	HAP	Powder metallurgy route that consists of mixing raw powders and consolidation by extrusion	The resistance to corrosion in PBS solution and the microhardness of the composites increased, the yield strength under compression slightly decreased
Deng et al. [153]	AZ91	SiCp	Stir casting technology then combination of forging and extrusion process	Tensile strength increased, plasticity at elevated temperatures improved
Zhong et al. [154]	Pure Mg	Alp	Powder metallurgy technique	Hardness, yield strength and ultimate tensile strength increased. The average ductility first decreased then increased
Habibnejad-Korayem et al. [155]	AZ31/Pure Mg	Alumina Al <sub>2</sub> O <sub>3</sub>	Stir-casting method	Yield stress and tensile strength increased the ductility decreased

**Table 2 – Mechanical properties of magnesium-ceramic composites.**

Sample	Processing route	Young's Modulus (GPa)	Tensile Properties			Compressive Properties			Grain size (µm)	Hardness (Hv)	Ref.	
			0.2%TYS (MPa)	UTS (MPa)	Ductility or Elongation (%)	CYS (MPa)	UCS (MPa)	Failure strain (%)				
Mg	Disintegrated melt deposition technique followed by hot extrusion	-	92 ± 5	156 ± 6	8.2 ± 0.2	57 ± 3	332 ± 10	18	45 ± 2.4	52 ± 1.5	[113]	
Mg-0.58TiO <sub>2</sub>		-	80 ± 2	128 ± 3	10 ± 0.5	78 ± 5	285 ± 13	22.6 ± 1	37 ± 3.6	58 ± 2		
Mg-0.97TiO <sub>2</sub>		-	97 ± 3	154 ± 7	10.8 ± 1	85.5 ± 2	278.4 ± 8	22.5 ± 1.5	29 ± 2	61 ± 2		
Mg-1.98TiO <sub>2</sub>		-	102 ± 3	165.5 ± 3	11.5 ± 1	88.3 ± 1	297 ± 1	21.9 ± 1	23 ± 5.5	64 ± 3		
Mg-2.5TiO <sub>2</sub>		-	124 ± 8.8	170 ± 6	10 ± 1	101 ± 9	305.5 ± 11	22 ± 2	21 ± 4	68 ± 1.5		
AZ91	Semi-solid stir casting	-	-	165	4.4	-	-	-	112.4	62 (HBW)	[156]	
AZ91-1.0TiB <sub>2</sub>		-	-	181	5.1	-	-	-	88.3	66 (HBW)		
AZ91-1.5TiB <sub>2</sub>		-	-	-	197	5.9	-	-	-	73.6	68 (HBW)	
AZ91-2.50TiB <sub>2</sub>		-	-	-	213	6.8	-	-	-	58.4	73 (HBW)	
ZK61	Spark plasma sintering	10.85	-	-	-	-	271 ± 6	13.6 ± 0.2	-	74.02	[32]	
ZK61-5β-TCP		10.51	-	-	-	-	338 ± 13	19.5 ± 0.6	-	83.54		
ZK61-10β-TCP		10.18	-	-	-	-	368 ± 5	18.3 ± 0.5	-	92.76		
ZK61-15β-TCP		10.67	-	-	-	-	402 ± 9	17.8 ± 0.3	-	94.81		
ZK60A	Powder metallurgy	37.1	245	279	-	-	-	-	-	-	[33]	
ZK60A--2.5CCP		41.9	264	285	-	-	-	-	-	-		
ZK60A--5CCP		45.6	322	340	-	-	-	-	-	-		
ZK60A-7.5CPP		44.1	267	305	-	-	-	-	-	-		
AZ91-SiCp (As-cast)	Stir casting	-	200	207	0.67	-	-	-	37.6	-	[138]	
AZ91-SiCp as-forged	Stir casting, then forging	-	243	282	1.06	-	-	-	9	-		
AZ91-SiCp (extruded)	Stir casting, then forging and extrusion	-	292	389	2.05	-	-	-	2.7	-		
Mg	Chemical synthesis process	-	124.1	187.9	-	-	-	-	27.5	31	[75]	
Mg-5HAp		-	122.3	171.1	-	-	-	-	-16.1	42		
Mg-10HAp		-	137.0	146.4	-	-	-	-	-14.9	55		
Mg-15HAp		-	129.6	136.7	-	-	-	-	-13.5	60		
Mg	Powder metallurgy	-	134 ± 7	193 ± 1	7.5 ± 2.5	-	-	-	20 ± 3	37 ± 2.0	[131]	
Mg-0.5Y <sub>2</sub> O <sub>3</sub>		-	144 ± 2	214 ± 4	8.0 ± 2.8	-	-	-	19 ± 3	38 ± 0.4		
Mg-2.0Y <sub>2</sub> O <sub>3</sub>		-	244 ± 1	244 ± 1	8.6 ± 1.2	-	-	-	18 ± 3	45 ± 2.0		
AZ91		Ultrasonic vibration	-	70	130	2.1	-	-	-	-	-	
AZ91-1 vol% SiCp		-	88	222	8.1	-	-	-	-	-	[157]	
AZ91	Remelting and dilution (RD) technique	45 ± 2	82 ± F3	233 ± 0	6.0 ± 0.5	-	-	-	-	-	[158]	
Mg-3.9 vol.% (TiB <sub>2</sub> +TiC)		53 ± 2	95 ± F2	298 ± 2	2.4 ± 0.4	-	-	-	-	-		
AZ91	Semisolid stirring assisted	-	70	125	1.9	-	-	-	-	-	[159]	
AZ91-SiCp stirring time:5 min	ultrasonic vibration	-	85	180	5.2	-	-	-	-	-		
AZ91-SiCp stirring time:10 min		-	107	162	2.2	-	-	-	-	-		
AZ91-SiCp stirring time:25 min		-	90	141	1.9	-	-	-	-	-		
AZ31B-1 vol.% SiCp	Semisolid stirring assisted	-	225	300	8.5	-	-	-	22	-	[160]	
AZ31B-2 vol.% SiCp	ultrasonic vibration	-	275	340	6.5	-	-	-	12	-		
AZ31B-3 vol.% SiCp	followed by hot extrusion	-	320	385	6.0	-	-	-	4.5	-		

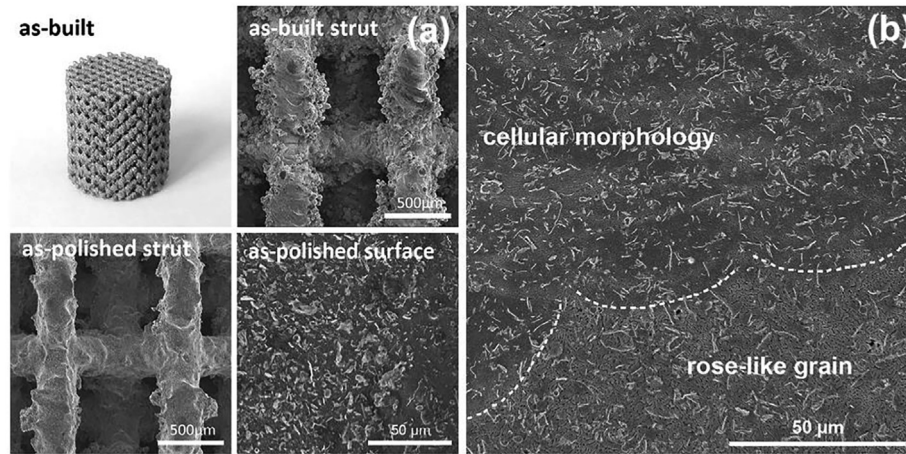
(continued on next page)



Table 2 – (continued)

Sample	Processing route	Young's Modulus (GPa)	Tensile Properties			Compressive Properties			Grain size ( $\mu\text{m}$ )	Hardness (Hv)	Ref.		
			0.2%TYS (MPa)	UTS (MPa)	Ductility or Elongation (%)	CYS (MPa)	UCS (MPa)	Failure strain (%)					
Mg	Melting and extrusion process	-	121.4	187.9	9.5	65.8	277.8	-	-	32	[161]		
Mg-5% HAp		-	-	-	-	-	-	-	-	42			
Mg-10% HAp		-	-	-	-	-	-	-	-	58			
Mg-15% HAp		-	129.6	136.7	0.3	147.1	298.2	-	-	67			
ZM61		-	195.7	301	14.7	141.2	355.6	-	-	68			
ZM61-5% HAp		-	-	-	-	-	-	-	-	78			
ZM61-10% HAp		-	-	-	-	-	-	-	-	89			
ZM61-15% HAp		-	225.5	225.5	0.3	245.3	388.3	-	-	94			
Mg	Powder metallurgy	-	134 $\pm$ 11	190 $\pm$ 10	4.6 $\pm$ 0.6	-	-	-	23 $\pm$ 6	46 $\pm$ 3	[154]		
Mg-0.25Alp		-	181 $\pm$ 14	221 $\pm$ 15	4.8 $\pm$ 0.4	-	-	-	17 $\pm$ 5	15HRT 54 $\pm$ 1			
Mg-0.50Alp		-	218 $\pm$ 16	271 $\pm$ 11	6.2 $\pm$ 0.9	-	-	-	17 $\pm$ 8	15HRT 57 $\pm$ 1			
Mg-0.75Alp		-	202 $\pm$ 7	261 $\pm$ 10	5.0 $\pm$ 1.6	-	-	-	16 $\pm$ 7	15HRT 60 $\pm$ 1			
Mg-1.00Alp		-	185 $\pm$ 9	226 $\pm$ 12	3.3 $\pm$ 1.0	-	-	-	16 $\pm$ 6	15HRT 61 $\pm$ 1			
Pure Mg		Melting and ultrasonic processing	-	20.0	89.6	14.0	-	-	-	-		-	[162]
Mg-0.5% SiC			-	28.3	120.7	15.5	-	-	-	-		-	
Mg-1% SiC			-	30.3	124.1	14.2	-	-	-	-		-	
Mg-2% SiC	-		35.9	131.0	12.6	-	-	-	-	-			
Mg-4% SiC	-	47.6	106.9	5.5	-	-	-	-	-	-			
Mg	Powder metallurgy, and conventional extrusion	-	-	-	-	189	296	0.09	37 $\pm$ 17	Hv(T):523 $\pm$ 5 (MPa)	[36]		
Mg-5HAp		-	-	-	-	202	329	0.10	30 $\pm$ 16	Hv(T):543 $\pm$ 7 (MPa)			
Mg-10HAp		-	-	-	-	205	334	0.13	41 $\pm$ 23	Hv(T):559 $\pm$ 7 (MPa)			
Mg-15HAp		-	-	-	-	207	348	0.14	27 $\pm$ 17	Hv(T):585 $\pm$ 8 (MPa)			
Mg	Powder metallurgy route that consists of mixing raw powders and consolidation by extrusion	-	-	-	-	224	340	0.131	-	Hv(L):490 $\pm$ 10MPa Hv(T):519 $\pm$ 5MPa	[35]		
Mg-5HAp		-	-	-	-	222	452	0.185	-	Hv(L):530 $\pm$ 10MPa Hv(T):560 $\pm$ 10MPa			
Mg-10HAp		-	-	-	-	219	415	0.175	-	Hv(L):580 $\pm$ 10MPa Hv(T):593 $\pm$ 7 MPa			
Mg-15HAp		-	-	-	-	216	371	0.223	-	H <sub>v</sub> (L):610 $\pm$ 10 (MPa) H <sub>v</sub> (T):623 $\pm$ 9 (MPa)			
Mg-3Zn	Powder processing route, using conventional sintering process	-	-	-	-	80 $\pm$ 1	130 $\pm$ 4	15 $\pm$ 1	-	340 (MPa)	[76]		
Mg-3Zn-2HAp		-	-	-	-	92 $\pm$ 3	131 $\pm$ 6	14 $\pm$ 1	-	350 (MPa)			
Mg-3Zn-5HAp		-	-	-	-	98 $\pm$ 4	134 $\pm$ 3	16 $\pm$ 1	-	370 (MPa)			
Mg-3Zn-10HAp		-	-	-	-	90 $\pm$ 2	116 $\pm$ 5	17 $\pm$ 1	-	480 (MPa)			
Mg	Disintegrated Melt Deposition technique followed by hot extrusion	37.5	92 $\pm$ 5	157 $\pm$ 5	8.2 $\pm$ 0.2	57 $\pm$ 3	332 $\pm$ 10	18	45 $\pm$ 2.4	52 $\pm$ 1.5	[163]		
Mg-1 vol% Ti		39.17	135 $\pm$ 3	197 $\pm$ 8	8.3 $\pm$ 0.6	130 $\pm$ 8	413 $\pm$ 15	18.5	2.5 $\pm$ 1.5	58 $\pm$ 1.5			
Mg-1vol% TiB <sub>2</sub>		38.06	110 $\pm$ 3	173 $\pm$ 8	16 $\pm$ 0.5	75 $\pm$ 7	333 $\pm$ 9	21 $\pm$ 1	28 $\pm$ 3.6	69 $\pm$ 2			
WZ73	Stir Casting Method	-	126 $\pm$ 13	172 $\pm$ 9	9 $\pm$ 1	-	-	-	143	77 $\pm$ 3	[164]		
WZ73-1.5 vol% SiC		-	160 $\pm$ 1	223 $\pm$ 8	6 $\pm$ 2	-	-	-	118	81 $\pm$ 9			
WZ73-2.5 vol% SiC		-	154 $\pm$ 9	238 $\pm$ 9	7 $\pm$ 1	-	-	-	114	79 $\pm$ 5			
Mg	Microwave sintering route	28	-	125	-	-	80	-	-	37.5	[165]		
Mg-5 wt% BG		36	-	190	-	-	100	-	-	44			
Mg-10 wt% BG		39	-	225	-	-	122	-	-	47.5			
Mg-15 wt%BG		34	-	180	-	-	110	-	-	49			

Note- TYS: Tensile yield strength, UTS: Ultimate tensile strength, CYS: Compressive yield strength, UCS: Ultimate compressive strength.



**Fig. 13 – Surface morphology, microstructure and composition analyses: (a) surface morphology on the periphery of WE43 scaffolds, (b) SEM image of melt pool [146].**

to the reinforcements via the interface of matrix reinforcement, and the strengthening happens because of the reinforcement's load transferring ability. Nevertheless, indirect strengthening occurs, whereas dislocations are produced in the MMCs by strain under external loads or because of a mismatch in the thermal expansion coefficient between matrix and particles. Furthermore, indirect strengthening occurs as a result of the Orowan mechanism and grain refinement process [23]. It was exhibited that under load, the matrix elongates, and the load is transmitted from the matrix to the particles via shear stress at the interface of the matrix reinforcement. The different coefficients of thermal expansion generate dislocations at the interface. The dislocation enhances the mechanical strength of MMCs. In such composites, Orowan strengthening is an effective strengthening mechanism [166]. Because of that, the Orowan looping can bypass the reinforcements. Therefore, the Orowan strengthening mechanism is more desirable in Mg-based composites with highly-dispersed nano-size reinforcements (smaller than 100 nm) even in the case of a minor volume fraction (<1%). For these composites, the increase in the yield stress as a result of Orowan looping is stated as follow [167]:

$$\Delta\sigma_{\text{Orowan}} = \frac{0.13G_m^b}{d_p \left[ (1/2v_p)^{1/3} - 1 \right]} \ln\left(\frac{d_p}{2b}\right) \quad (5)$$

where  $v_p$  and  $d_p$  are the volume fraction and diameter of the nano reinforcement, respectively,  $b$  and  $G$  are the Burgers vector and shear modulus of the matrix, respectively [61]. Furthermore, nanoparticles may obstruct glides of dislocation according to the Orowan effect, resulting in a significant improvement in strength [168]. Grain refinement is an important reason for improving the corrosion and mechanical characteristics. The well-known Hall–Petch relation describes grain refinement strengthening, which is stated as follow:

$$\sigma = \sigma_0 + kd^{-1/2} \quad (6)$$

where  $\sigma$  is the yield strength,  $\sigma_0$  a material constant,  $k$  is the coefficient of strengthening and  $d$  is the average diameter of grain [40]. In this regard, Yang et al. [67] proposed grain

refinement as another viable counteraction to enhance the toughness and strength because the grain boundaries are a strong barrier against slipping of the dislocation. Similarly, it was reported that grain refinement and precipitation of secondary phases in Mg matrix play an important role in enhancing the mechanical properties. The degradation and mechanical properties of Mg-based composites are directly influenced by the alloying components, type of reinforcement, and manufacturing processes [40]. The appropriate alloying-reinforcement of Mg-based biocomposites for suitable orthopedic implants must be determined [40]. The research conducted by Deng et al. [169] demonstrated that a combination of micron and submicron particles had a considerable favorable effect on grain refinement and increasing mechanical characteristics. Furthermore, they revealed the method of strengthening micron and submicron particles reinforced Mg-based composite [62,170]. As previously stated, a reduction in grain size and increase in volume fraction can significantly increase the Orowan effect and dislocation strengthening. Because of the low volume fraction of nanoparticles supplied, the load transfer mechanism contributes little. Therefore, to enhance nanocomposites' operation, a high amount of nano-size reinforcement with further secondary deformation can be added. This could enhance the Orowan looping effect, load-bearing mechanism, and grain refinement strengthening if the added reinforcements are dispersed uniformly in the Mg matrix [61]. For example, the adding of nano alumina reinforcements increased the AZ31B alloy's yield strength through the Orowan strengthening effect and the precipitation hardening strengthening mechanism. Furthermore, MMC with reinforcing particles of  $\text{Al}_2\text{O}_3$ ,  $\text{ZrO}_2$ , calcium phosphate  $\text{Ca}_3(\text{PO}_4)_2$ , or yttria ( $\text{Y}_2\text{O}_3$ ) are suitable options to improve the mechanical properties of Mg matrix [40,171]. Cui et al. [37] reported adding the amount of hard ceramic particles-HA in the Mg-5.5Zn/HAp composite improved mechanical characteristics, which might be attributable to two mechanisms. Firstly, geometrically necessary dislocations (GNDs): incompatibility in plastic deformation might increase mechanical characteristics of MMCs. The mismatch in thermal expansion coefficient and shear modulus ( $G$ ) between Mg matrix and HAp

reinforcements is the reason behind this. Therefore, residual stresses caused by heating appear between Mg and HAp and lead to form a substantial amount of GNDs in the Mg-5.5Zn/HAp composite. The formation of the dislocation enhances the composite's tensile strength [76,172]. Secondly, there is a work hardening mechanism because of the generation of dislocations and strain mismatch between the nanofillers and the matrix [32]. The addition of HAp to the Mg-3Zn/HAp composite enhances its hardness. The increment in composite hardness in comparison with Mg-3Zn alloy could be attributable to the cumulative effect of strain hardening caused by the existence of reinforcements of varied sizes and phases in the Mg-3Zn/HAp composite. They also discovered that the incorporation of HAp particles into the matrix helped to the limitation of dislocation movement. Dislocations are the principal species responsible for work hardening. These reinforcements serve as pinning points, preventing dislocation movement. The uniform distribution of HAp particles provides pinning action that prevents the twinning phenomena. This could illustrate why the Mg-Zn/HAp composites have a higher yield strength [76]. Similarly, due to the reinforcing influence of inorganic fillers, a BG-10/Mg composite will have better mechanical properties than a pure Mg. However, the decreased ductility of Mg/BG composites in comparison with the pure Mg is mostly due to the existence of inorganic fillers in the matrix that caused the limitation of plastic deformation [165]. So, the grain refinement, the secondary phases, incorporating the reinforcements into the matrix, and the manufacturing process are the main reasons to improve mechanical properties [13]. In conclusion, manufacturing conditions such as casting, powder metallurgy, and other severe plastic deformation processes have a major impact on grain refinement and matrix strengthening [40].

The presence of hard particles in a metallic matrix increases strength while decreasing ductility. Construction of bi-modal grain microstructures by adding coarse grains to the matrix is one technique for increasing the ductility of composites. Because of their considerably higher strain hardening capability, coarse grains enable deformation ability. Randomly distributed zones, on the other hand, have little effectiveness in preventing crack propagation and can even promote strain localization [173]. Zan et al. [174] proposed a heterogeneous structural strategy for composites with good strength and ductility synergy. Among the heterogeneous structures, the lamella structure, which consists of lamellar soft zones embedded in a hard matrix, is projected to provide more efficient ductility improvement with high strength. They reported that the composite with the lamella structure improved both strength and ductility compared to composites with the uniform ultrafine grained (UFG) structure or the random bi-modal grain structure. Sankaranarayanan et al. [175] demonstrated the effects of nano-B<sub>4</sub>C addition and heat treatment on the mechanical characteristics of Mg-(5.6Ti+3Al) systems, claiming that the addition of nano-B<sub>4</sub>C particulates to Mg-(5.6Ti+3Al) provided improved ductility and strength retention, which was attributed to the combined presence of nano-B<sub>4</sub>C and Al<sub>3</sub>Ti intermetallic phases in Mg matrix. The interfacial stress reduction between the matrix and the other secondary phases/reinforcements

were attributable to the significant improvement in ductility. Furthermore, the presence of uniformly dispersed nanoparticles metallic oxide would improve ductility via grain boundary pinning [125]. Rashad et al. [176] claimed that refined grain size and uniformly dispersed reinforcing particles increased the ductility of tested Mg nanocomposite. Hassan et al. [177] summarized the other reason that contributes to the rise of ductility of reinforced Mg nanocomposites at high thermal-activation of non-basal slip systems. The intensity of texture changed at increasing temperatures as some of the crystallites with <1010> direction rotated away from the compressive axis due to the slip of second-order pyramidal slip systems. When this slip is restricted due to the presence of nano reinforcements, prismatic and basal slip systems are activated [125,178].

## 7. In vitro corrosion behavior

To simulate the corrosion properties of biodegradable metals in vivo, several in vitro corrosion tests have been developed. The conditions must be as similar to in vivo as possible. In vivo, the corrosive environment includes a 0.14 M NaCl solution with low concentrations of other inorganic compounds such as Ca<sup>2+</sup>, PO<sub>4</sub><sup>3-</sup>, and HCO<sub>3</sub><sup>-</sup>. In most cases, the existence of Cl<sup>-</sup> ions speeds up corrosion, while PO<sub>4</sub><sup>3-</sup> and HCO<sub>3</sub><sup>-</sup> ions can form the corrosion product as a protective layer. Furthermore, temperature, pH, amino acids, cells, or protein may affect corrosion reactions. The temperature in the human body and blood pH are 37 °C and 7.4, respectively. The researchers have reported that Mg(OH)<sub>2</sub> is the important corrosion product of Mg implants in vitro and in vivo. Figure 14 [69] illustrates the various interactions with the corroding Mg alloy surface. The chemical reactions that occur during the corrosion process are as follows [179,180]:



The high amount of Cl<sup>-</sup> ion in body fluid lessens this protective oxide layer and accelerates the degradation rate of Mg alloys. As the process continues, calcium phosphate deposition on the metal oxide layer is caused by saturated calcium and phosphate in the body fluid and local alkalization, which allows cells to attach to the surface and form tissues [69]. Corrosion in vitro simulates an in vivo degradable process via a collection of in vitro techniques such as weight-loss analysis, hydrogen evolution testing and electrochemical analysis [181]. To design an appropriate simulated in vitro method [182]; a) as an electrolyte solution, buffered SBF with components similar to those found in human blood must be used, b) surface roughness of the specimens should be similar to implants to minimize the error, c) due to the in vivo condition following the cell adhesion, immersion time should be decreased and d) surface area to volume ratio of the solution

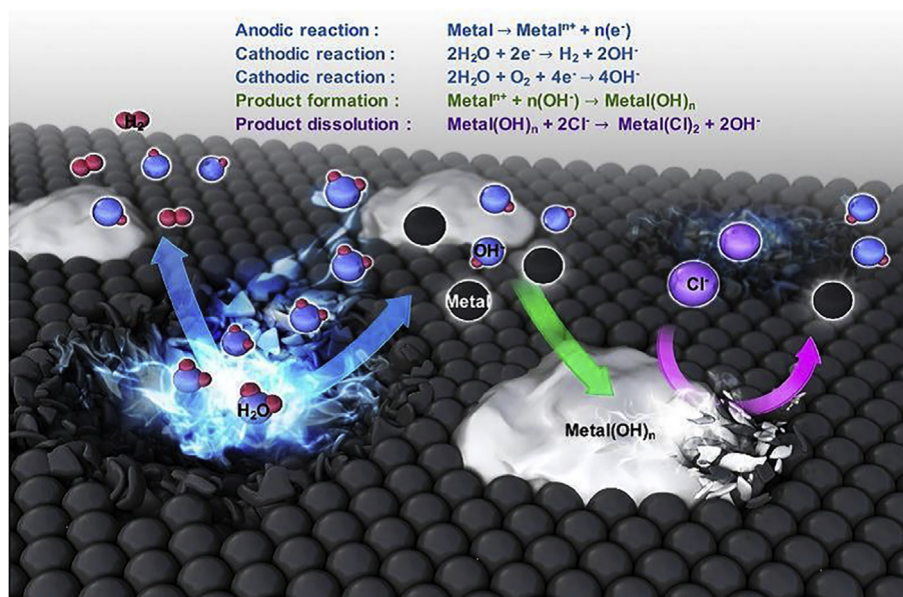


Fig. 14 – Corrosion/degradation behavior in physiological environment with production of various corrosion products [69].

and the rate of fluid flow must be close to the in vivo conditions.

The studies [25,128,183,184] have revealed that there is an optimal content of each type of ceramic reinforcement for improving corrosion characteristics. For example, less than 10 wt. % HAp is recommended for use in the matrix because higher concentrations of HAp tend to form large clusters or agglomeration in metal matrices, resulting in non-uniform degradation, and studies have shown that the presence of more than 10 wt. % HAp in this composite showed non-uniform HAp distribution, leading to uneven corrosion in the composite. When compared to HAp, TCP reinforcement has a faster degradation rate. However, excessive aggregation of TCP particles due to their low wettability with the matrix might lead to unequal and faster corrosion in biological conditions. According to Zheng et al. [185], the corrosion resistance of the composite decreases as the Ca particle content increases. Furthermore, corrosion resistance increased considerably during the initial immersion stage and remained steady after that. After 12 h of immersion, the surface film composition of the three Mg/Ca composite samples remained nearly constant. The surface treatment can also be used to provide a physical barrier to separate the underlying Mg matrix from corrosive fluid and assist in the mechanical integrity of Mg implants prior to complete healing. Surface treatment is a viable strategy for controlling the deterioration rate of Mg-based implants. Su et al. [186] used a simple conversion coating technique to fabricate biocompatible dicalcium phosphate dihydrate (DCPD) and HAp coatings on homemade HAp/Mg composites in an attempt to improve the corrosion resistance and surface biocompatibility of the composites in order to meet the desired requirements of biomedical applications. Electrochemical and immersion experiments revealed that the optimal coatings, particularly the HAp coating, greatly decreased the composites' degradation rate in SBF.

Since each method of calculating corrosion rates has advantages and disadvantages, they can complete each other. Studies have reported that the corrosion rate of a Mg implant in vitro condition (immersion test) is comparable to in vivo studies (implantation into rat femurs), because their rate of degradation was nearly identical [187,188]. It has been found that the presence of reinforcing nanoparticles in the Mg matrix improves corrosion resistance [61]. Dutta et al. [88] have produced Mg/xBG ( $x = 0, 5, 10$  and  $15$  wt%) composites via a hot-press sintering procedure. In vitro corrosion studies of Mg/xBG composites revealed that Mg/10% BG had the best corrosion behavior. Feng et al. [33] used hot extrusion after hot pressing to create ZK60A-CPP composites. In vitro results demonstrated that incorporating calcium polyphosphate into the ZK60A matrix increased the composite's corrosion resistance. The existence of  $\text{Ca}^{2+}$  ion in the product of degradation and stable  $\text{Mg}(\text{OH})_2$  on the specimen surface caused the improved corrosion properties of ZK60A-CPP composites [33]. Also, another study of in vitro corrosion on the AZ91/fluorapatite nanocomposite represented that, altering the composition lead to facilitate the creation of a protective apatite layer on the sample surface [59]. Ye et al. [189] studied the biocompatibility and in vitro corrosion resistance and of the Mg composites reinforced with nano HAp and discovered that Mg-HAp nanocomposites had better corrosion behavior than MgZrZn alloys.

Razavi et al. [73] produced an Mg/FAp nanocomposite via blending–pressing–sintering method. The electrochemical polarization curves of the AZ91 alloy and AZ91/FA composites in Ringer solution at  $37^\circ\text{C}$  and the pure Mg and Mg-BG composites in PBS at  $37^\circ\text{C}$ . The existence of the ceramics nanoparticles with better corrosion resistance at the Mg matrix grain boundary led to the corrosion resistance of the composites improved [59,73,76,88]. Also, the rate of apatite layer formation can be accelerated by adding reinforcements into

the composites. On the other hand, the anodic behavior of Mg and creation of the galvanic coupling between the reinforcement and matrix or interfacial reaction products cause a slight decrease in corrosion resistance [76,88,180].

Bakhsheshi rad et al. [190] developed Mg–Ca–TiO<sub>2</sub> (MCT) composite scaffolds with porosities and pore sizes ranging from 65 to 67% and 600–800 μm, respectively. The bioactivity results revealed the production of apatite on the MCT scaffold surface. The formation of bone-like apatite on the surface of the scaffolds is a crucial component of bone-biomaterial integration, causing the scaffolds to remain in place after implantation [191]. Increased porosity promotes cell attachment, proliferation, differentiation, and tissue ingrowth, resulting in improved bone regeneration [191,192] but it compromises corrosion resistance and mechanical characteristics. Porous scaffolds with a typical pore size greater than 300 μm can provide a superior physiological environment for cell proliferation and tissue growth [26,27].

For the first time, Lespinasse [193] stated a difference between *in vivo* and *in vitro* corrosion of Mg and they noted that the corrosion of Mg-based implant in sodium chloride rich solution would be faster than in water [47]. Recent Mg corrosion studies have found that, due to a lack of knowledge of Mg bio-corrosion, the rate of corrosion evaluated *in vitro* is higher than the rate of corrosion measured *in vivo* [13]. Lin et al. [194] exhibited that an *in vitro* and *in vivo* correlation (IVIVC) has a crucial function in developing novel materials to aid in the protection of animals and to shorten the time process of *in vivo* studies. However, the IVIVC requires further study by the researchers. For the comparison of *in vitro* and *in vivo* study results, a standard technique is required to specify how certain parameters affect the *in vitro* corrosion of the specimens [195,196]. Generally, many studies have reported that the existence of the different reinforcements can change the corrosion rate of Mg-ceramic composites. Depending on the manufacturing procedure, the composites and type of the matrix and reinforcements material, the corrosion rate can increase or decrease. The corrosion rate with various fabrication methods, corrosion medium and the properties of the measurement process reported in various studies are collected in Table 3. In summary, Fig. 15 demonstrates the corrosion behavior of Mg in all of the previously stated media [197]. NaCl solution could be utilized for preliminary screening tests for alloy choice and corrosion behavior. In comparison to conventional NaCl solution, the corrosion resistance of metallic substrates in simulated body fluids (e.g., SBF, HBSS, EBSS) is lower. SBF can also be utilized as a primary screening test. Cell culture medium including MEM, DMEM, and M199, whereas a protein-containing solution is a proper choice to study the corrosion behavior of biomaterial. This solution is so close to the blood plasma environment and can also be utilized to study corrosion behavior for the development of implants [197].

## 8. In vitro biocompatibility

According to studies, due to the reaction of bone cells to pure Mg and lost mechanical integrity of the pure Mg in a

physiological environment, the pure Mg implant application is limited. As a result, bioactive particle reinforced Mg composites are being developed. The widespread use of Mg-ceramic composites in medical applications such as the used stents in the heart and orthopedic applications shows *in vitro* biocompatibility of these composites is so considerable. Many studies have demonstrated that Mg composites have superior biocompatibility when compared to other metallic metal composites [85]. All composite components in Mg implants must be nontoxic and biocompatible in the physiological condition [25]. The metallic ions produced by the corrosion of biodegradable Mg implants can cause toxicity in the human body [13]. In general, if each element used exceeds its threshold limit, it can cause toxicity in the body [199,200]. As a result, choosing the element plays an important role in increasing biocompatibility in biological conditions. Furthermore, the selection of solution volume and pH is so important factor in determining *in vitro* biocompatibility. *In vitro* methods used to analyze the biocompatibility of biomaterials are a critical step in evaluating the potential safety of the implants for medical application [42]. Coagulation and platelet aggregation are evaluated *in vitro* biocompatibility of Mg-ceramic composites for cardiovascular applications like stents [201], and cell culture is used for orthopedic implants in accordance with ISO 10993–5 and ISO 10993-12 standards to study *in vitro* biocompatibility of Mg-ceramic composites [202,203]. According to studies, there is an indirect technique that the cultured cells are exposed to a material extract for various periods of time, and in the second technique, the material and the cultured cells are in direct contact [42]. Both of these techniques are used to test the viability of cells. Due to the excellent biocompatibility and non-toxicity of Mg, it has emerged as a suitable choice for degradable load-bearing orthopedic implants [204]. The studies have shown that the biocompatibility of Mg-based implants is related to corrosion resistance [83,201,205]. Mostly during the degradation of Mg-based composites, particular particles or cations from the reinforcement are being released, enhancing bioactivity [206–210]. Kumar et al. [151] have produced AZ31-Al<sub>2</sub>O<sub>3</sub> nanocomposites via an advanced disintegrated melt deposition (DMD) process followed by hot extrusion to increase the corrosion resistance and *in vitro* biocompatibility in simulated body fluid (SBF). According to the reports of the *in vitro* biocompatibility tests, the corrosion layer includes an amorphous Mg(OH)<sub>2</sub>, MgAl<sub>2</sub>O<sub>4</sub>, and apatite-like layer, which improves the bioactivity of the AZ31/Al<sub>2</sub>O<sub>3</sub> nanocomposite. Several researchers have asserted that incorporation of the reinforcements into the matrix increased cell proliferation and viability of the cell while decreasing corrosion rates [206]. Jaiswal et al. [76] reported that HAP reinforcements facilitate the growth of the apatite layer. In this regard, they found by increasing immersion time, more apatite layer was noticed in the Mg–3Zn–HA biodegradable composites. They have stated that the Mg–HAp composite is an excellent choice for orthopedic fracture fixing products [76]. The *in vitro* cytotoxic results indicated improved cell growth, cell proliferation, and well-formed spindle shape cell morphology, as shown in Fig. 16 [180].

A 0.14 M NaCl solution with small concentrations of other inorganic components such as Ca<sup>2+</sup>, PO<sub>4</sub><sup>3-</sup>, and HCO<sub>3</sub><sup>-</sup> makes

**Table 3 – Corrosion properties of magnesium-ceramic composites.**

matrix	Reinforcement	Processing Route	Corrosion Medium	$i_{corr}$ ( $\mu A.cm^{-2}$ )	$E_{corr}$ (V vs. SCE)	Corrosion Rate (mm/year)			Rp	Ref.	
						Non Polarized		Polarized			
						Immersion Time (h)	HE or WL	PDP			
AZ31	–	Innovative disintegrated melt deposition (DMD) process followed by hot extrusion	SBF	9.470	–1.545	1	2.176	–	–	[151]	
				4.422	–1.441	24	1.016	–	–		
				21.345	–1.402	336	4.906	–	–		
				2.552	–1.472	1	0.586	–	–		
				0.786	–1.402	24	0.180	–	–		
AZ31	Al <sub>2</sub> O <sub>3</sub>			1.863	–1.392	336	0.428	–	–		
				1.742	–1.408	24	0.400	–	–		
				0.933	–1.373	336	0.214	–	–		
				–	–	100	23	–	–		
				–	–	–	15	–	–		
Mg	–	Powder metallurgy route that consists of mixing raw powders and consolidation by extrusion	PBS	–	–	–	24	–	–	[35]	
				–	–	–	60	–	–		
				–	–	–	–	–	–		
				–	–	–	–	–	–		
Mg	–	Spark plasma sintering method	Hank's	27	–1.63	–	–	–	–	[152]	
				ZnO (10 wt %)	3.0	–1.50	–	–	–		–
				ZnO (20 wt %)	30	–1.59	–	–	–		–
				ZnO (10 wt %)	2.2	–1.47	–	–	–		–
				ZnO (20 wt %)	8	–1.57	–	–	–		–
Mg	–	Sintering in Vacuum Furnace before spark plasma sintering method	PBS	167	–1527	168	19.35	3.82	–	[88]	
				Hot press sintering	13.28	–1.47	–	3.44	0.30		–
					5.71	–1.37	–	2.84	0.13		–
					27.84	–1.42	–	12.30	0.64		–
Mg	–	Microwave sintering route	SBF	–	–	4	0.016 ml/mm <sup>2</sup> /h	–	–	[165]	
				–	–	–	0.004 ml/mm <sup>2</sup> /h	–	–		
				–	–	–	0.01 ml/mm <sup>2</sup> /h	–	–		
				–	–	–	0.005 ml/mm <sup>2</sup> /h	–	–		
				–	–	8	0.06 ml/mm <sup>2</sup> /h	–	–		
				–	–	–	0.054 ml/mm <sup>2</sup> /h	–	–		
				–	–	–	0.045 ml/mm <sup>2</sup> /h	–	–		
				–	–	–	0.025 ml/mm <sup>2</sup> /h	–	–		
				–	–	16	0.065 ml/mm <sup>2</sup> /h	–	–		
				–	–	–	0.055 ml/mm <sup>2</sup> /h	–	–		
				–	–	–	0.050 ml/mm <sup>2</sup> /h	–	–		
				–	–	–	0.040 ml/mm <sup>2</sup> /h	–	–		
				ZK60A	–	Powder metallurgy	SBF	0.116	–1.60		–
0.092	–1.58	–	–					–	–		
0.088	–1.56	–	–					–	–		
0.077	–1.52	–	–					–	–		
Mg–Zn–Zr	–	Casting followed by extrosion	SBF	–	–1.630	480	1.64	–	1630 $\Omega$	[189]	
				HA	–	–1.615	–	0.75	–		2560 $\Omega$

(continued on next page)

Table 3 – (continued)

matrix	Reinforcement	Processing Route	Corrosion Medium	$i_{corr}$ ( $\mu\text{A}\cdot\text{cm}^{-2}$ )	$E_{corr}$ (V vs. SCE)	Corrosion Rate (mm/year)		Rp	Ref.
						Polarized			
						Non Polarized	PDP		
Immersion Time (h)		HE or WL	PDP						
Mg–3Zn	–	Powder processing route, using conventional sintering process	SBF	$962.41 \pm 2.16$	$-1.78 \pm 0.025$	–	–	–	[76]
	HAp (2%wt)			$777.02 \pm 3.77$	$-1.76 \pm 0.060$	–	–	–	
	HAp (5%wt)			$571.97 \pm 4.17$	$-1.65 \pm 0.020$	–	–	–	
	HAp (10%wt)			$682.16 \pm 4.97$	$-1.69 \pm 0.022$	–	–	–	
WZ73	–	Stir casting method	1 wt % NaCl	–	–	24	16	–	[164]
	1.5 vol % SiC			–	–	27	–	–	
	2.5 vol % SiC			–	–	25	–	–	
AZ91E	–	Powder metallurgy	3.5% NaCl	0.880	–0.98	15	–	–	[198]
	TiC			0.002	–1.39	–	–	–	
Mg	–	Disintegrated Melt Deposition technique followed by hot extrusion	Dulbecco's Modified Eagle's Medium (DMEM) + 10% FBS + 1% Penicillin	–	–	48	0.6890	–	[163]
	~1 vol.% TiB <sub>2</sub>			–	–	120	129.87	–	
	–			–	–	–	0.5512	–	
	~1 vol.% Ti			–	–	–	0.3415	–	
	–			–	–	240	0.2756	–	
	~1 vol.% Ti			–	–	–	0.1366	–	

Note:  $i_{corr}$ : corrosion current density,  $E_{corr}$ : corrosion potentials, HE: hydrogen evolution, WL: weight loss, PDP:potentio-dynamic polarization, Rp: polarization resistance.

the corrosive media of the human body. The normal pH of blood is 7.4, which is buffered by the  $\text{CO}_2/\text{HCO}_3^-$  system. The presence of organic components such as biomolecules, proteins, cells, or bacteria, in addition to the variety of inorganic species found in body fluids, can influence corrosion reactions. The Mg surface attracts cells and proteins, and cells on the surface generate lactic acid.  $\text{Mg}^{2+}$  cations can be complexed by proteins in solution [180].

## 9. In vivo degradation and compatibility

In vivo implantation is required to characterize the corrosion behavior of MMnCs in physiological settings properly. The procedures used to assess Mg corrosion after in vivo implantation is linked with measuring the physical reduction in the size of the materials caused by corrosion that happened during the implantation period. The most prevalent of these procedures is micro-computed tomography analysis of the remaining volume of the implanted material. The assessment of the implant's weight loss is another method used to analyze the corrosion of Mg materials in vivo. The examination of the residual cross-sectional area of the implants in two-dimensional parts is the only other quantitative method utilized to assess Mg corrosion in vivo [211–213].

Zhou et al. [212] investigated the in vivo degradation and compatibility of a 5-TCP/Mg–3Zn scaffold with polydopamine/gelatin (PDA/G) composite coatings. This sample's electrochemical tests when compared to bare 5-TCP/Mg–3Zn alloy, the corrosion current density ( $i_{corr}$ ) decreased from  $5.24 \times 10^{-3}$  to  $1.41 \times 10^{-3}$  A/cm<sup>2</sup>, suggesting superior anti-corrosion capabilities. The in vivo tests revealed that the materials and coatings were harmless to muscle and other critical organs such as the heart, liver, kidney, and muscle. The in vivo release of  $\text{Mg}^{2+}$  was identified because it is one of the methods used to assess degradation and cytotoxicity. From pre-surgery to 2 months after implantation, the serum concentration of Mg ion was greater in the bare sample than in the PDA/G coated sample, attributed to the rapid degradation of the Mg substrate. In-vivo biodegradation findings demonstrated normal morphology with no cell degeneration or necrosis and no inflammatory cell infiltration in the tissue, showing that the alloy, composite coating, and degradation products were highly biocompatible.

Yu et al. [213] used PM to manufacture a Mg-6% Zn–15%  $\text{Ca}_3(\text{PO}_4)_2$  composite. Metal ion concentrations in rabbit blood were measured, and liver, heart, kidney, and muscle tissues were examined for morphological analysis. The results demonstrated that the  $\text{Ca}^{2+}$ ,  $\text{Zn}^{2+}$ , and  $\text{Mg}^{2+}$  ions in the animal's blood were within normal limits throughout the experiment. All of the tissues remained normal during the composite degradation procedure, indicating that the composite was biocompatible with the sevisceral organs.

To increase corrosion resistance and bone response, Chen et al. [211] developed composite coatings with HAp, octacalcium phosphate (OCP) in electrochemical deposition (ED) layers and MgO,  $\text{Mg}_3(\text{PO}_4)_2$  in micro-arc oxidation (MAO) layers on Mg–Zn–Ca alloy by ED and MAO. In vivo testing revealed that the coated samples degraded far more slowly than the substrates. In the pathological evaluation, the

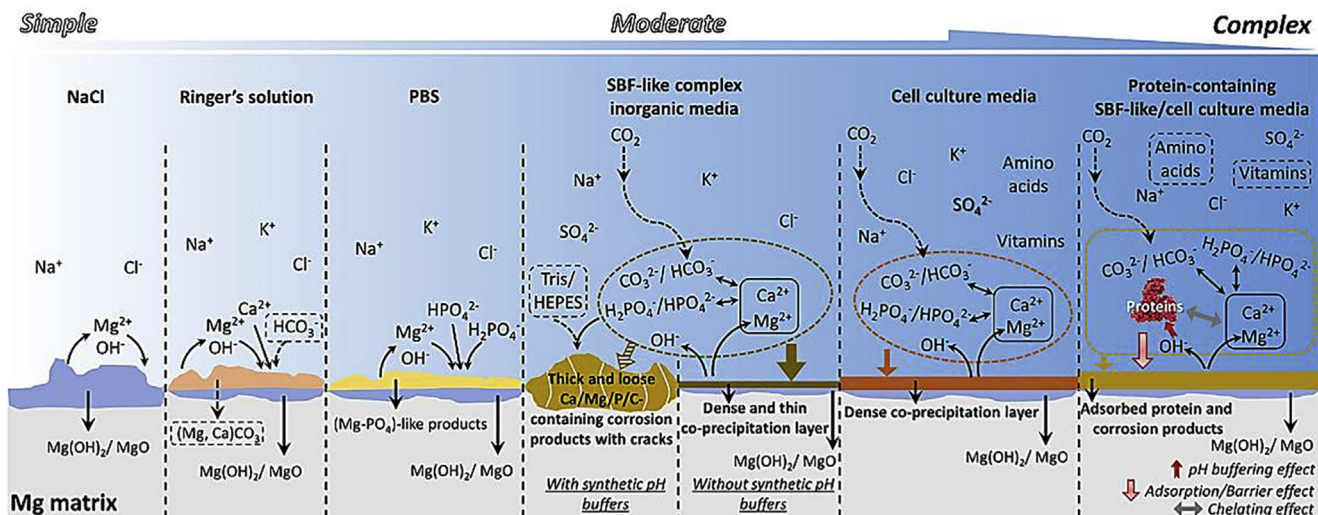


Fig. 15 – Schematic illustration of the corrosion behavior of Mg in the commonly used media [197].

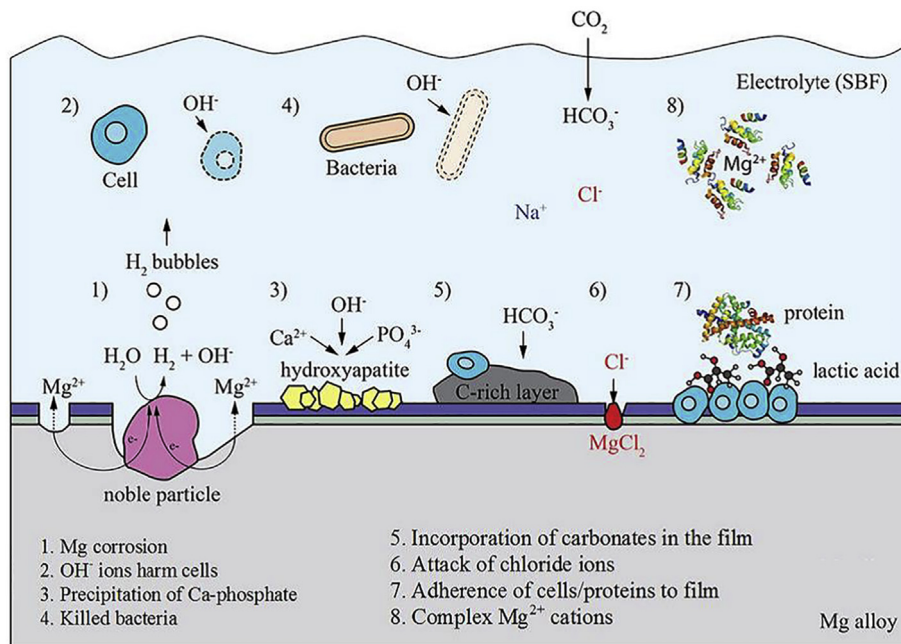


Fig. 16 – Schematic of the interactions between a corroding magnesium alloy and a biological environment [180].

composite coatings stopped the Mg substrates from rapidly degrading and presented good bioactivity.

Besides, scientists around the world are becoming increasingly concerned about the toxicity of nano additions in vivo [194,212,213]. The toxicity of nanoparticles is debatable and depends on the susceptibility of the cell type, route of exposure, and condition, and the features of the nanoparticles. Mahmoud et al. [214] investigated the toxicity of MgO nanoparticles from the liver (HepG2), kidney (NRK-52E), intestine (Caco-2), and lung (A549) cell lines. They discovered that whereas MgO nanoparticles generated apoptotic effects on the cells, apoptosis was not the primary cause of cell death. The effects of MgO nanoparticles on DNA damage, cell death, and oxidative damage should raise concerns regarding the

safety of their use in consumer products. Zhao et al. [215] evaluated the feasibility of using pure Mg screws for the fixation of vascularized bone grafts in patients with osteonecrosis of the femoral head (ONFH). According to the findings, the Mg screw is biocompatible and efficient in bone flap stabilization. Its degradation rate is acceptable in comparison to the rate of tissue repair, and the released Mg ions promote new bone production. Wu et al. [56] investigated the possibility of biodegradable Mg alloys for use in tracheal stents. The researchers discovered that Mg alloys (magnesium-aluminum-zinc-calcium-manganese (AZXM)) had outstanding cytocompatibility and that AZXM is a promising candidate for tracheal stent applications. According to Gu et al. [216] the as-rolled Mg–2Sr alloy exhibited Grade I



cytotoxicity and produced more alkaline phosphatase activity than the other alloys. They observed steady degradation of the as-rolled Mg–2Sr alloy inside a bone tunnel over a 4-week period of implantation [216]. Microcomputer tomography and histological examination revealed increased mineral density and thicker cortical bone around the experimental implants. However, more research will be required before Mg-based composites can be used as orthopedic implants, such as illustrating the absence of systemic toxicity (e.g., organ pathology), particularly after long-term implantation, as well as improving mechanical characteristics and further lessening the corrosion rate.

## 10. Conclusions

Due to the widespread use of magnesium-ceramic composites for orthopedic implants, their properties and applications, with a focus on the requirements for Mg composite development, commonly used reinforcement materials, fabrication methods, in vitro corrosion, and in vitro biocompatibility, were reviewed. The importance of Mg and its alloys and composites as bone implants has been confirmed. The advantages of Mg-ceramic composites are the inherent biodegradability, favorable mechanical properties, and biocompatibility. Recent studies have shown that the appropriate selection of ceramic reinforcements such as hydroxyapatite (HAp), fluorapatite (FAp), Zirconium oxide ( $ZrO_2$ ), titanium dioxide ( $TiO_2$ ), magnesium oxide (MgO), zinc oxide (ZnO), bioactive glass (BG), calcium polyphosphate particles (CPP), bredigite (Bre), and aluminium oxide ( $Al_2O_3$ ) and their inherent biocompatible nature is so important as these reinforcements can have a significant effect on the properties and applications of Mg-based biocomposites. Various studies on the fabrication techniques of these implants, including powder metallurgy, casting, wrought techniques, and laser additive manufacturing were expressed. Laser additive manufacturing facilitates the rapid production of complicated porous structures or customized shapes compared with traditional fabricating methods. Several studies results have shown that the presence of reinforcements usually improves mechanical performance, in vitro corrosion resistance and biocompatibility of Mg composites. Selecting the most efficient process for in vitro corrosion and in vitro biocompatibility of Mg composites is critical, and more investigation is necessary in this area.

Several methods [217–222] have been developed to overcome the issues of corrosion and the low yield strength of pure Mg. This review focuses on recent advances in Mg-based composites with bioactive reinforcements for biological applications. Controlled degradation with appropriate mechanical integrity, on the other hand, is a significant difficulty for these materials. Researchers [35,83,85,90,99] used bioactive and biodegradable additions such as calcium polyphosphate, bioactive glass, and fluorapatite to achieve controlled degradation. A considerable number of works [31,35,152,183,212] in the literature demonstrated that including these additions in Mg composites could modify their corrosion resistance and give good biocompatibility for

use as metallic biomaterials in bone tissue engineering applications. The size and distribution of reinforcements significantly affect the modulation of the composite's corrosion resistance and mechanical characteristics. Additionally, a study on biodegradable Mg-based composites for fracture repair implants has resulted in significantly innovative product manufacturing. Mg composites with specific mechanical and corrosion properties can be created using advanced methods, including hot press sintering, spark plasma sintering, disintegrated melt deposition, and laser additive manufacturing. In general, improvements in Mg alloy manufacturing techniques, as well as the selection of appropriate reinforcement are vital for extending the biomedical uses of Mg-based composites. Degradable Mg composites with a good combination of mechanical characteristics and degradation rate could be the focus of future research. Immersion and electrochemical experiments were used to study the degradation of Mg composites in vitro. It was expected that homogeneous reinforcement distribution would increase the composite's corrosion resistance [57,62,163]. Nondestructive micro-computed tomography (CT) should be used to investigate the distribution of reinforcements in the matrix, as well as their influence on electrochemical corrosion and in vitro degradation. With the aid of CT analysis, the corrosion pit depth on the sample surface can be accurately measured, and it represents an appropriate evaluation of corrosion resistance. CT research can provide shed light on the corrosion mechanism of biodegradable composites. An orthopedic device is subjected to both tensile and compressive loading during use, requiring sufficient tensile strength and ductility. The majority of the existing literature [32,35,76] on degradable Mg composites has reported the compressive strength of composites. Only a few have reported on the composites' tensile strength and ductility. Mg has an HCP crystal structure with a low slip system and thus limited ductility. The ductility of the Mg matrix is further reduced when reinforcements are added. To properly realize the benefits of these newly established Mg composites, it is crucial to evaluate their tensile properties. Recent research on Mg-based degradable composites [44,83,88,90,152,185,205] has been limited to in vitro degradation and cytocompatibility tests. The study of in vivo degradation behavior may lead to a new field of research. In vitro investigations of degradable Mg composites show an increased immunogenic response, which has to be confirmed in vivo. Furthermore, new research frontiers should be truly tested. In this regard, it is worth noting that the majority of in vivo investigations involving Mg-based biomaterials were carried out in small animal models, and the findings are difficult to interpret for human applications. In this regard, it is worth noting that the majority of in vivo investigations involving Mg-based biomaterials were carried out in small animal models, and the findings are difficult to interpret for human applications. To thoroughly study the potential of –Mg-based biomaterials (MBs) as orthopedic devices and better understand their long-term in-vivo performance, more experimental investigation in large animal models, particularly at load-bearing application sites, is required before preclinical and clinical trials.

## Declaration of Competing Interest

The authors declare that they have no known competing financial interests or personal relationships that could have appeared to influence the work reported in this paper.

## Abbreviations

MMCs	Metal matrix composites
MMnCs	Metal matrix nanocomposites
Mg	Magnesium
SS	Stainless steel
HAp	Hydroxyapatite
CPP	Calcium polyphosphate
Bre	Bredigite
BG	Bioactive glass
MBG	mesoporous bioglass
$\beta$ -TCP	Beta-tricalcium phosphate
FA	Fluorapatite
LAM	Laser additive manufacturing
AM	Additive manufacturing
SBF	Simulated body fluid
BG	Bioglass
PM	Powder metallurgy
DMD	Disintegrated melt deposition
SPM	Semi-powder metallurgy
SLM	Selective laser melting
UTS	Ultimate tensile strength
TS	Tensile strength
TYS	Tensile yield strength
E	Elastic modulus
UCS	Ultimate compressive strength
CYS	Compressive yield strength
CTE	Coefficient of thermal expansion
SPS	Spark plasma sintering
DMEM	Dulbecco's Modified Eagle's Medium
Icorr	Corrosion current density
Ecorr	Corrosion potentials
HE	Hydrogen evolution
WL	Weight loss
PDP	Potential-dynamic polarization
R <sub>p</sub>	Polarization resistance
MW	microwave sintering
GNDs	geometrically necessary dislocations
HBSS	Hank's Balanced Salt Solution
EBSS	Earle's Balanced Salt Solution
MEM	Minimum Essential Medium
DMEM	Dulbecco's Modified Eagle Medium
$\alpha$ -MEM	Minimum Essential Medium $\alpha$
M199	Medium 199

## REFERENCES

- [1] Gao C, Peng S, Feng P, Shuai C. Bone biomaterials and interactions with stem cells. *Bone Res* 2017;5:1–33.
- [2] Hanawa T. Research and development of metals for medical devices based on clinical needs. *Sci Technol Adv Mater* 2012;13:64102.
- [3] Jariwala SH, Lewis GS, Bushman ZJ, Adair JH, Donahue HJ. 3D printing of personalized artificial bone scaffolds. *3D Print Addit Manuf* 2015;2:56–64.
- [4] Bhattacharjee P, Kundu B, Naskar D, Kim H-W, Maiti TK, Bhattacharya D, et al. Silk scaffolds in bone tissue engineering: an overview. *Acta Biomater* 2017;63:1–17.
- [5] Nomoto H, Maehashi H, Shirai M, Nakamura M, Masaki T, Mezaki Y, et al. Bio-artificial bone formation model with a radial-flow bioreactor for implant therapy—comparison between two cell culture carriers: porous hydroxyapatite and  $\beta$ -tricalcium phosphate beads. *Hum Cell* 2019;32:1–11.
- [6] Ibrahim CZ, Sarhan AAD, Kuo TY, Hamdi M, Yusof F, Chien CS, et al. Advancement of the artificial amorphous-crystalline structure of laser cladded FeCrMoCB on nickel-free stainless-steel for bone-implants. *Mater Chem Phys* 2019;227:358–67.
- [7] Kurian M, Stevens R, McGrath KM. Towards the development of artificial bone grafts: combining synthetic biomineralisation with 3D printing. *J Funct Biomater* 2019;10:12.
- [8] Park J, Lakes RS. *Biomaterials: an introduction*. Springer Science & Business Media; 2007.
- [9] Sunil BR, Dumpala R. Magnesium-based composites for degradable implant applications. *Encyclopedia of Materials: Composites* 2021;2:770–80.
- [10] Hedayati R, Ahmadi SM, Lietaert K, Tümer N, Li Y, Amin Yavari S, et al. Fatigue and quasi-static mechanical behavior of biodegradable porous biomaterials based on magnesium alloys. *J Biomed Mater Res* 2018;106:1798–811.
- [11] Teoh SH. Fatigue of biomaterials: a review. *Int J Fatig* 2000;22:825–37.
- [12] Katz JL. Anisotropy of Young's modulus of bone. *Nature* 1980;283:106–7.
- [13] Ali M, Hussein MA, Al-Aqeeli N. Magnesium-based composites and alloys for medical applications: a review of mechanical and corrosion properties. *J Alloys Compd* 2019;792:1162–90.
- [14] Long PH. Medical devices in orthopedic applications. *Toxicol Pathol* 2008;36:85–91.
- [15] Peron M, Torgersen J, Berto F. Mg and its alloys for biomedical applications: exploring corrosion and its interplay with mechanical failure. *Metals* 2017;7:252.
- [16] Hanawa T. Overview of metals and applications. In: *Met. Biomed. Devices*. Elsevier; 2019. p. 3–29.
- [17] Lendlein A, Rehahn M, Buchmeiser MR, Haag R. Polymers in biomedicine and electronics. *Macromol Rapid Commun* 2010;31:1487–91.
- [18] Pruitt L, Furmanski J. Polymeric biomaterials for load-bearing medical devices. *JOM (J Occup Med)* 2009;61:14–20.
- [19] Dubok VA. Bioceramics yesterday, today, tomorrow. *Powder Metall. Met. Ceram.* 2000;39:381–94.
- [20] Hench LL. Bioceramics: from concept to clinic. *J Am Ceram Soc* 1991;74:1487–510.
- [21] Ramakrishna S, Mayer J, Wintermantel E, Leong KW. Biomedical applications of polymer-composite materials: a review. *Compos Sci Technol* 2001;61:1189–224.
- [22] Wang M. Bioactive ceramic-polymer composites for tissue replacement. In: *Eng. Mater. Biomed. Appl.* World Scientific; 2004. p. 1–8.
- [23] Dutta S, Gupta S, Roy M. Recent developments in magnesium metal–matrix composites for biomedical applications: a review. *ACS Biomater Sci Eng* 2020;6:4748–73.
- [24] Zheng YF, Gu XN, Witte F. Biodegradable metals. *Mater Sci Eng R Rep* 2014;77:1–34.
- [25] Bommala VK, Krishna MG, Rao CT. Magnesium matrix composites for biomedical applications: a review. *J. Magnes. Alloy.* 2019;7:72–9.

- [26] Xiong G, Nie Y, Ji D, Li J, Li C, Li W, et al. Characterization of biomedical hydroxyapatite/magnesium composites prepared by powder metallurgy assisted with microwave sintering. *Curr Appl Phys* 2016;16:830–6.
- [27] Jayasathyakawin S, Ravichandran M, Baskar N, Chairman CA, Balasundaram R. Magnesium matrix composite for biomedical applications through powder metallurgy—Review. *Mater. Today Proc.* 2020;27:736–41.
- [28] Raman RKS, Jafari S, Harandi SE. Corrosion fatigue fracture of magnesium alloys in bioimplant applications: a review. *Eng Fract Mech* 2015;137:97–108.
- [29] Ghasali E, Alizadeh M, Niazmand M, Ebadzadeh T. Fabrication of magnesium-boron carbide metal matrix composite by powder metallurgy route: comparison between microwave and spark plasma sintering. *J Alloys Compd* 2017;697:200–7.
- [30] Höhn S, Virtanen S, Boccaccini AR. Protein adsorption on magnesium and its alloys: a review. *Appl Surf Sci* 2019;464:212–9.
- [31] Kiani F, Wen C, Li Y. Prospects and strategies for magnesium alloys as biodegradable implants from crystalline to bulk metallic glasses and composites—a review. *Acta Biomater* 2020;103:1–23.
- [32] Cui Z, Zhang Y, Cheng Y, Gong D, Wang W. Microstructure, mechanical, corrosion properties and cytotoxicity of beta-calcium polyphosphate reinforced ZK61 magnesium alloy composite by spark plasma sintering. *Mater Sci Eng C* 2019;99:1035–47.
- [33] Feng A, Han Y. Mechanical and in vitro degradation behavior of ultrafine calcium polyphosphate reinforced magnesium-alloy composites. *Mater Des* 2011;32:2813–20.
- [34] Witte F, Feyerabend F, Maier P, Fischer J, Störmer M, Blawert C, et al. Biodegradable magnesium–hydroxyapatite metal matrix composites. *Biomaterials* 2007;28:2163–74.
- [35] Del Campo R, Savoini B, Muñoz A, Monge MA, Garcés G. Mechanical properties and corrosion behavior of Mg–HAP composites. *J. Mech. Behav. Biomed. Mater.* 2014;39:238–46.
- [36] Del Campo R, Savoini B, Muñoz A, Monge MA, Pareja R. Processing and mechanical characteristics of magnesium-hydroxyapatite metal matrix biocomposites. *J. Mech. Behav. Biomed. Mater.* 2017;69:135–43.
- [37] Cui Z, Li W, Cheng L, Gong D, Cheng W, Wang W. Effect of nano-HA content on the mechanical properties, degradation and biocompatible behavior of Mg-Zn/HA composite prepared by spark plasma sintering. *Mater Char* 2019;151:620–31.
- [38] Wang X, Zhang P, Dong LH, Ma XL, Li JT, Zheng YF. Microstructure and characteristics of interpenetrating  $\beta$ -TCP/Mg–Zn–Mn composite fabricated by suction casting. *Mater Des* 2014;54:995–1001.
- [39] He S-Y, Yue SUN, Chen M-F, Liu D-B, Ye X-Y. Microstructure and properties of biodegradable  $\beta$ -TCP reinforced Mg-Zn-Zr composites. *Trans Nonferrous Metals Soc China* 2011;21:814–9.
- [40] Radha R, Sreekanth D. Insight of magnesium alloys and composites for orthopedic implant applications—a review. *J. Magnes. Alloy.* 2017;5:286–312.
- [41] Yang Y, He C, Dianyu E, Yang W, Qi F, Xie D, et al. Mg bone implant: features, developments and perspectives. *Mater Des* 2020;185:108259.
- [42] Walker J, Shadanbaz S, Woodfield TBF, Staiger MP, Dias GJ. Magnesium biomaterials for orthopedic application: a review from a biological perspective. *J Biomed Mater Res B Appl Biomater* 2014;102:1316–31.
- [43] Bettman RB, Zimmerman LM. The use of metal clips in gastrointestinal anastomosis. *Am J Dig Dis* 1935;2:318–21.
- [44] Zhou H, Liang B, Jiang H, Deng Z, Yu K. Magnesium-based biomaterials as emerging agents for bone repair and regeneration: from mechanism to application. *J. Magnes. Alloy* 2021;9:779–804.
- [45] Song J, She J, Chen D, Pan F. Latest research advances on magnesium and magnesium alloys worldwide. *J. Magnes. Alloy.* 2020;8:1–41.
- [46] Seelig MG. A study of magnesium wire as an absorbable suture and ligature material. *Arch Surg* 1924;8:669–80.
- [47] Witte F. The history of biodegradable magnesium implants: a review. *Acta Biomater* 2010;6:1680–92.
- [48] Riaz U, Shabib I, Haider W. The current trends of Mg alloys in biomedical applications—a review. *J Biomed Mater Res B Appl Biomater* 2019;107:1970–96.
- [49] Andrews EW. Absorbable metal clips as substitutes for ligatures and deep sutures in wound closure. *J Am Med Assoc* 1917;69:278–81.
- [50] Jorgensen R. Bio absorbable metal hemostatic clip. 1986.
- [51] Chen Y, Xu Z, Smith C, Sankar J. Recent advances on the development of magnesium alloys for biodegradable implants. *Acta Biomater* 2014;10:4561–73.
- [52] Yun Y, Dong Z, Yang D, Schulz MJ, Shanov VN, Yarmolenko S, et al. Biodegradable Mg corrosion and osteoblast cell culture studies. *Mater Sci Eng C* 2009;29:1814–21.
- [53] Ibrahim H, Esfahani SN, Poorganji B, Dean D, Elahinia M. Resorbable bone fixation alloys, forming, and post-fabrication treatments. *Mater Sci Eng C* 2017;70:870–88.
- [54] Lock JY, Wyatt E, Upadhyayula S, Whall A, Nunez V, Vullev VI, et al. Degradation and antibacterial properties of magnesium alloys in artificial urine for potential resorbable ureteral stent applications. *J Biomed Mater Res* 2014;102:781–92.
- [55] Wang S, Zhang X, Li J, Liu C, Guan S. Investigation of Mg–Zn–Y–Nd alloy for potential application of biodegradable esophageal stent material. *Bioact. Mater.* 2020;5:1–8.
- [56] Wu J, Lee B, Saha P, Kumta PN. A feasibility study of biodegradable magnesium-aluminum-zinc-calcium-manganese (AZXM) alloys for tracheal stent application. *J Biomater Appl* 2019;33:1080–93.
- [57] Kuśnierzcyk K, Basista M. Recent advances in research on magnesium alloys and magnesium–calcium phosphate composites as biodegradable implant materials. *J Biomater Appl* 2017;31:878–900.
- [58] Sezer N, Evis Z, Kayhan SM, Tahmasebifar A, Koç M. Review of magnesium-based biomaterials and their applications. *J. Magnes. Alloy.* 2018;6:23–43.
- [59] Razavi M, Fathi MH, Meratian M. Microstructure, mechanical properties and bio-corrosion evaluation of biodegradable AZ91-FA nanocomposites for biomedical applications. *Mater Sci Eng* 2010;527:6938–44.
- [60] Abazari S, Shamsipur A, Bakhsheshi-Rad HR, Ramakrishna S, Berto F. Graphene family nanomaterial reinforced magnesium-based matrix composites for biomedical application: a comprehensive review. *Metals* 2020;10:1002.
- [61] Nie KB, Wang XJ, Deng KK, Hu XS, Wu K. Magnesium matrix composite reinforced by nanoparticles—a review. *J. Magnes. Alloy* 2021;9:57–77.
- [62] Deng K, Wang X, Wang C, Shi J, Hu X, Wu K. Effects of bimodal size SiC particles on the microstructure evolution and fracture mechanism of AZ91 matrix at room temperature. *Mater Sci Eng* 2012;553:74–9.
- [63] Haghshenas M. Mechanical characteristics of biodegradable magnesium matrix composites: a review. *J. Magnes. Alloy.* 2017;5:189–201.

- [64] Khorashadizade F, Saghafeian H, Rastegari S. Effect of electrodeposition parameters on the microstructure and properties of Cu-TiO<sub>2</sub> nanocomposite coating. *J Alloys Compd* 2019;770:98–107.
- [65] Khayat S, Fanaei H, Ghanbarzahi A. Minerals in pregnancy and lactation: a review article. *J. Clin. Diagnostic Res. JCDR* 2017;11:QE01.
- [66] Chng CB, Lau DP, Choo JQ, Chui CK. A bioabsorbable microclip for laryngeal microsurgery: design and evaluation. *Acta Biomater* 2012;8:2835–44.
- [67] Yang Y, Wang G, Liang H, Gao C, Peng S, Shen L, et al. Additive manufacturing of bone scaffolds. *Int. J. Bioprinting* 2019;5.
- [68] Staiger MP, Kolbeinson I, Kirkland NT, Nguyen T, Dias G, Woodfield TBF. Synthesis of topologically-ordered open-cell porous magnesium. *Mater Lett* 2010;64:2572–4.
- [69] Han H-S, Loffredo S, Jun I, Edwards J, Kim Y-C, Seok H-K, et al. Current status and outlook on the clinical translation of biodegradable metals. *Mater Today* 2019;23:57–71.
- [70] Dezfuli SN, Leeflang S, Huan Z, Chang J, Zhou J. Advanced bredigite-containing magnesium-matrix composites for biodegradable bone implant applications. *Mater Sci Eng C* 2017;79:647–60.
- [71] Khodaei M, Nejatidanesh F, Shirani MJ, Valanezhad A, Watanabe I, Savabi O. The effect of the nano-bioglass reinforcement on magnesium based composite. *J. Mech. Behav. Biomed. Mater.* 2019;100:103396.
- [72] Bolokang AS, Motaung DE, Arendse CJ, Camagu ST, Muller TFG. Structure–property analysis of the Mg–TiO<sub>2</sub> and Mg–Sn–TiO<sub>2</sub> composites intended for biomedical application. *Mater Lett* 2015;161:328–31.
- [73] Razavi M, Fathi MH, Meratian M. Fabrication and characterization of magnesium–fluorapatite nanocomposite for biomedical applications. *Mater Char* 2010;61:1363–70.
- [74] Kwon S-H, Jun Y-K, Hong S-H, Kim H-E. Synthesis and dissolution behavior of  $\beta$ -TCP and HA/ $\beta$ -TCP composite powders. *J Eur Ceram Soc* 2003;23:1039–45.
- [75] Khanra AK, Jung HC, Yu SH, Hong KS, Shin KS. Microstructure and mechanical properties of Mg-HAP composites. *Bull Mater Sci* 2010;33:43–7.
- [76] Jaiswal S, Kumar RM, Gupta P, Kumaraswamy M, Roy P, Lahiri D. Mechanical, corrosion and biocompatibility behaviour of Mg-3Zn-HA biodegradable composites for orthopaedic fixture accessories. *J. Mech. Behav. Biomed. Mater.* 2018;78:442–54.
- [77] Nakahata I, Tsutsumi Y, Kobayashi E. Mechanical properties and corrosion resistance of magnesium–hydroxyapatite composites fabricated by spark plasma sintering. *Metals* 2020;10:1314.
- [78] Khalil KA, Sherif E-SM, Almajid AA. Corrosion passivation in simulated body fluid of magnesium/hydroxyapatite nanocomposites sintered by high frequency induction heating. *Int. J. Electrochem. Sci.* 2011;6:6184–99.
- [79] Khalajabadi SZ, Kadir MRA, Izman S, Ebrahimi-Kahrizsangi R. Fabrication, bio-corrosion behavior and mechanical properties of a Mg/HA/MgO nanocomposite for biomedical applications. *Mater Des* 2015;88:1223–33.
- [80] Yu X, Tang X, Gohil SV, Laurencin CT. Biomaterials for bone regenerative engineering. *Adv. Healthc. Mater.* 2015;4:1268–85.
- [81] Zheng H, Li Z, Chen M, You C, Liu D. The effect of nano  $\beta$ -TCP on hot compression deformation behavior and microstructure evolution of the biomedical Mg-Zn-Zr alloy. *Mater Sci Eng* 2018;715:205–13.
- [82] Zheng HR, Li Z, You C, Liu DB, Chen MF. Effects of MgO modified  $\beta$ -TCP nanoparticles on the microstructure and properties of  $\beta$ -TCP/Mg-Zn-Zr composites. *Bioact Mater* 2017;2:1–9.
- [83] Huan Z, Leeflang S, Zhou J, Zhai W, Chang J, Duszczyc J. In vitro degradation behavior and bioactivity of magnesium-Bioglass® composites for orthopedic applications. *J Biomed Mater Res B Appl Biomater* 2012;100:437–46.
- [84] Jones JR. Review of bioactive glass: from Hench to hybrids. *Acta Biomater* 2013;9:4457–86.
- [85] Dutta S, Devi KB, Gupta S, Kundu B, Balla VK, Roy M. Mechanical and in vitro degradation behavior of magnesium-bioactive glass composites prepared by SPS for biomedical applications. *J Biomed Mater Res B Appl Biomater* 2019;107:352–65.
- [86] El-Rashidy AA, Roether JA, Harhaus L, Kneser U, Boccaccini AR. Regenerating bone with bioactive glass scaffolds: a review of in vivo studies in bone defect models. *Acta Biomater* 2017;62:1–28.
- [87] Hench LL. Opening paper 2015–some comments on bioglass: four eras of discovery and development. *Biomed Glas* 2015;1.
- [88] Dutta S, Devi KB, Mandal S, Mahato A, Gupta S, Kundu B, et al. In vitro corrosion and cytocompatibility studies of hot press sintered magnesium-bioactive glass composite. *Materialia* 2019;5:100245.
- [89] Yang Y, Lu C, Shen L, Zhao Z, Peng S, Shuai C. In-situ deposition of apatite layer to protect Mg-based composite fabricated via laser additive manufacturing. *J Magnes Alloy* 2021.
- [90] Yin Y, Huang Q, Liang L, Hu X, Liu T, Weng Y, et al. In vitro degradation behavior and cytocompatibility of ZK30/bioactive glass composites fabricated by selective laser melting for biomedical applications. *J Alloys Compd* 2019;785:38–45.
- [91] Yang Y, Peng S, Tian Z, Shuai C. Copper-doped mesoporous bioactive glass endows magnesium based scaffold with antibacterial activity and corrosion resistance. *Mater Chem Front* 2021.
- [92] Driessens FCM. Probable phase composition of the mineral in bone. *Z Naturforsch C Biosci* 1980;35:357–62.
- [93] Su J, Teng J, Xu Z, Li Y. Biodegradable magnesium-matrix composites: a review. *Int J Miner Metall Mater* 2020;27:724–44.
- [94] Jackson LE, Kariuki BM, Smith ME, Barralet JE, Wright AJ. Synthesis and structure of a calcium polyphosphate with a unique criss-cross arrangement of helical phosphate chains. *Chem Mater* 2005;17:4642–6.
- [95] Porter NL, Pilliar RM, Grynblas MD. Fabrication of porous calcium polyphosphate implants by solid freeform fabrication: a study of processing parameters and in vitro degradation characteristics. *J. Biomed Mater Res An Off J Soc Biomater Japanese Soc Biomater Aust Soc Biomater Korean Soc Biomater* 2001;56:504–15.
- [96] Grynblas MD, Pilliar RM, Kandel RA, Renlund R, Filiaggi M, Dumitriu M. Porous calcium polyphosphate scaffolds for bone substitute applications in vivo studies. *Biomaterials* 2002;23:2063–70.
- [97] Kim H-W, Kim H-E, Knowles JC. Fluor-hydroxyapatite sol–gel coating on titanium substrate for hard tissue implants. *Biomaterials* 2004;25:3351–8.
- [98] Fathi MH, Zahrani EM. Fabrication and characterization of fluoridated hydroxyapatite nanopowders via mechanical alloying. *J Alloys Compd* 2009;475:408–14.
- [99] Fathi MH, Zahrani EM. Mechanical alloying synthesis and bioactivity evaluation of nanocrystalline fluoridated hydroxyapatite. *J Cryst Growth* 2009;311:1392–403.
- [100] Sirelkhatim A, Mahmud S, Seeni A, Kaus NHM, Ann LC, Bakhori SKM, et al. Review on zinc oxide nanoparticles:

- antibacterial activity and toxicity mechanism. *Nano-Micro Lett* 2015;7:219–42.
- [101] Laurenti M, Cauda V. ZnO nanostructures for tissue engineering applications. *Nanomaterials* 2017;7:374.
- [102] Lei T, Tang W, Cai S-H, Feng F-F, Li N-F. On the corrosion behaviour of newly developed biodegradable Mg-based metal matrix composites produced by in situ reaction. *Corrosion Sci* 2012;54:270–7.
- [103] Selvam B, Marimuthu P, Narayanasamy R, Anandakrishnan V, Tun KS, Gupta M, et al. Dry sliding wear behaviour of zinc oxide reinforced magnesium matrix nano-composites. *Mater Des* 2014;58:475–81.
- [104] Tun KS, Jayaramanavar P, Nguyen QB, Chan J, Kwok R, Gupta M. Investigation into tensile and compressive responses of Mg–ZnO composites. *Mater Sci Technol* 2012;28:582–8.
- [105] Wu C, Chang J. Synthesis and in vitro bioactivity of bredigite powders. *J Biomater Appl* 2007;21:251–63.
- [106] Yi D, Wu C, Ma B, Ji H, Zheng X, Chang J. Bioactive bredigite coating with improved bonding strength, rapid apatite mineralization and excellent cytocompatibility. *J Biomater Appl* 2014;28:1343–53.
- [107] Wu C, Chang J, Wang J, Ni S, Zhai W. Preparation and characteristics of a calcium magnesium silicate (bredigite) bioactive ceramic. *Biomaterials* 2005;26:2925–31.
- [108] Lei T, Ouyang C, Tang W, Li L-F, Zhou L-S. Enhanced corrosion protection of MgO coatings on magnesium alloy deposited by an anodic electrodeposition process. *Corrosion Sci* 2010;52:3504–8.
- [109] Goh CS, Gupta M, Wei J, Lee LC. Characterization of high performance Mg/MgO nanocomposites. *J Compos Mater* 2007;41:2325–35.
- [110] Lin G, Liu D, Chen M, You C, Li Z, Wang Y, et al. Preparation and characterization of biodegradable Mg-Zn-Ca/MgO nanocomposites for biomedical applications. *Mater Char* 2018;144:120–30.
- [111] Shuai C, Wang B, Bin S, Peng S, Gao C. Interfacial strengthening by reduced graphene oxide coated with MgO in biodegradable Mg composites. *Mater Des* 2020:108612.
- [112] Pc E, Radhakrishnan G, Emarose S. Investigation into physical, microstructural and mechanical behaviour of titanium dioxide nanoparticulate reinforced magnesium composite. *Mater Technol* 2021;36:575–84.
- [113] Meenashisundaram GK, Nai MH, Almajid A, Gupta M. Development of high performance Mg–TiO<sub>2</sub> nanocomposites targeting for biomedical/structural applications. *Mater Des* 2015;65:104–14.
- [114] Khaled Sm, Sui R, Charpentier PA, Rizkalla AS. Synthesis of TiO<sub>2</sub>–PMMA nanocomposite: using methacrylic acid as a coupling agent. *Langmuir* 2007;23:3988–95.
- [115] Khosroshahi HK, Saniee FF, Abedi HR. Mechanical properties improvement of cast AZ80 Mg alloy/nanoparticles composite via thermomechanical processing. *Mater Sci Eng* 2014;595:284–90.
- [116] Qiao K, Zhang T, Wang K, Yuan S, Zhang S, Wang L, et al. Mg/ZrO<sub>2</sub> metal matrix nanocomposites fabricated by friction stir processing: microstructure, mechanical properties, and corrosion behavior. *Front Bioeng Biotechnol* 2021;9:197.
- [117] Navazani M, Dehghani K. Fabrication of Mg-ZrO<sub>2</sub> surface layer composites by friction stir processing. *J Mater Process Technol* 2016;229:439–49.
- [118] Vaira Vignesh R, Padmanaban R, Govindaraju M, Suganya Priyadharshini G. Investigations on the corrosion behaviour and biocompatibility of magnesium alloy surface composites AZ91D-ZrO<sub>2</sub> fabricated by friction stir processing. *Trans IMF* 2019;97:261–70.
- [119] Hassan SF, Gupta M. Effect of nano-ZrO<sub>2</sub> particulates reinforcement on microstructure and mechanical behavior of solidification processed elemental Mg. *J Compos Mater* 2007;41:2533–43.
- [120] Hassan SF, Tan MJ, Gupta M. Development of nano-ZrO<sub>2</sub> reinforced magnesium nanocomposites with significantly improved ductility. *Mater Sci Technol* 2007;23:1309–12.
- [121] Hassan SF, Gupta M. Effect of different types of nano-size oxide particulates on microstructural and mechanical properties of elemental Mg. *J Mater Sci* 2006;41:2229–36.
- [122] Rahmani K, Majzoobi GH, Sadooghi A, Kashfi M. Mechanical and physical characterization of Mg-TiO<sub>2</sub> and Mg-ZrO<sub>2</sub> nanocomposites produced by hot-pressing. *Mater Chem Phys* 2020;246:122844.
- [123] Rahmani K, Nouri A, Wheatley G, Malekmohammadi H, Bakhtiari H, Yazdi V. Determination of tensile behavior of hot-pressed Mg–TiO<sub>2</sub> and Mg–ZrO<sub>2</sub> nanocomposites using indentation test and a holistic inverse modeling technique. *J Mater Res Technol* 2021;14:2107–14.
- [124] Nguyen QB, Gupta M. Microstructure and mechanical characteristics of AZ31B/Al<sub>2</sub>O<sub>3</sub> nanocomposite with addition of Ca. *J Compos Mater* 2009;43:5–17.
- [125] Song X, Bayati P, Gupta M, Elahinia M, Haghshenas M. Fracture of magnesium matrix nanocomposites-a review. *Int J Light Mater Manuf* 2021;4:67–98.
- [126] Gupta M, Wong WLE. Magnesium-based nanocomposites: lightweight materials of the future. *Mater Char* 2015;105:30–46.
- [127] Annur D, Suhardi A, Amal MI, Anwar MS, Kartika I. Powder metallurgy preparation of Mg-Ca alloy for biodegradable implant application. In: *J. Phys. Conf. Ser. IOP Publishing*; 2017. p. 12062.
- [128] Shahin M, Munir K, Wen C, Li Y. Magnesium matrix nanocomposites for orthopedic applications: a review from mechanical, corrosion, and biological perspectives. *Acta Biomater* 2019;96:1–19.
- [129] Kumar A, Pandey PM. Development of Mg based biomaterial with improved mechanical and degradation properties using powder metallurgy. *J Magnes Alloy* 2020;8:883–98.
- [130] Li X, Ma G, Jin P, Zhao L, Wang J, Li S. Microstructure and mechanical properties of the ultra-fine grained ZK60 reinforced with low content of nano-diamond by powder metallurgy. *J Alloys Compd* 2019;778:309–17.
- [131] Tun KS, Gupta M. Improving mechanical properties of magnesium using nano-yttria reinforcement and microwave assisted powder metallurgy method. *Compos Sci Technol* 2007;67:2657–64.
- [132] Ghasali E, Bordbar-Khiabani A, Alizadeh M, Mozafari M, Niazmand M, Kazemzadeh H, et al. Corrosion behavior and in-vitro bioactivity of porous Mg/Al<sub>2</sub>O<sub>3</sub> and Mg/Si<sub>3</sub>N<sub>4</sub> metal matrix composites fabricated using microwave sintering process. *Mater Chem Phys* 2019;225:331–9.
- [133] Ali Y, Qiu D, Jiang B, Pan F, Zhang M-X. The influence of CaO addition on grain refinement of cast magnesium alloys. *Scripta Mater* 2016;114:103–7.
- [134] Radhamani AV, Lau HC, Ramakrishna S. CNT-reinforced metal and steel nanocomposites: a comprehensive assessment of progress and future directions. *Compos Part A Appl Sci Manuf* 2018;114:170–87.
- [135] Abazari S, Shamsipur A, Bakhsheshi-Rad HR, Ismail AF, Sharif S, Razzaghi M, et al. Carbon nanotubes (CNTs)-Reinforced magnesium-based matrix composites: a comprehensive review. *Materials* 2020;13:4421.
- [136] Ho KF, Gupta M, Srivatsan TS. The mechanical behavior of magnesium alloy AZ91 reinforced with fine copper particulates. *Mater Sci Eng* 2004;369:302–8.

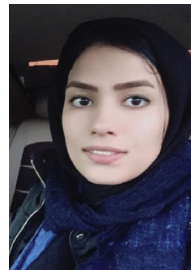
- [137] Cao F, Shi Z, Song G-L, Liu M, Dargusch MS, Atrens A. Influence of hot rolling on the corrosion behavior of several Mg–X alloys. *Corrosion Sci* 2015;90:176–91.
- [138] Wu K, Deng K, Nie K, Wu Y, Wang X, Hu X, et al. Microstructure and mechanical properties of SiCp/AZ91 composite deformed through a combination of forging and extrusion process. *Mater Des* 2010;31:3929–32.
- [139] Munsch M. Laser additive manufacturing of customized prosthetics and implants for biomedical applications. In: *Laser addit. Manuf.* Elsevier; 2017. p. 399–420.
- [140] Gu D. Laser additive manufacturing of high-performance materials. Springer; 2015.
- [141] Liu F-H, Shen Y-K, Liao Y-S. Selective laser gelation of ceramic–matrix composites. *Compos B Eng* 2011;42:57–61.
- [142] Zhou S, Dai X. Microstructure evolution of Fe-based WC composite coating prepared by laser induction hybrid rapid cladding. *Appl Surf Sci* 2010;256:7395–9.
- [143] Gu D, Ma J, Chen H, Lin K, Xi L. Laser additive manufactured WC reinforced Fe-based composites with gradient reinforcement/matrix interface and enhanced performance. *Compos Struct* 2018;192:387–96.
- [144] Ng CC, Savalani MM, Man HC, Gibson I. Layer manufacturing of magnesium and its alloy structures for future applications. *Virtual Phys Prototyp* 2010;5:13–9.
- [145] Brånemark R, Emanuelsson L, Palmquist A, Thomsen P. Bone response to laser-induced micro- and nano-size titanium surface features. *Nanomed Nanotechnol Biol Med* 2011;7:220–7.
- [146] Li Y, Zhou J, Pavanram P, Leeftang MA, Fockaert LI, Pouran B, et al. Additively manufactured biodegradable porous magnesium. *Acta Biomater* 2018;67:378–92.
- [147] Xu R, Zhao M-C, Zhao Y-C, Liu L, Liu C, Gao C, et al. Improved biodegradation resistance by grain refinement of novel antibacterial ZK30-Cu alloys produced via selective laser melting. *Mater Lett* 2019;237:253–7.
- [148] Yang Y, Lu C, Peng S, Shen L, Wang D, Qi F, et al. Laser additive manufacturing of Mg-based composite with improved degradation behaviour. *Virtual Phys Prototyp* 2020;15:278–93.
- [149] Shuai C, Zhou Y, Yang Y, Feng P, Liu L, He C, et al. Biodegradation resistance and bioactivity of hydroxyapatite enhanced Mg–Zn composites via selective laser melting. *Materials* 2017;10:307.
- [150] Karunakaran R, Ortgies S, Tamayol A, Bobaru F, Sealy MP. Additive manufacturing of magnesium alloys. *Bioact. Mater.* 2020;5:44–54.
- [151] Kumar AM, Hassan SF, Sorour AA, Paramsothy M, Gupta M. Electrochemical corrosion and in vitro biocompatibility performance of AZ31Mg/Al<sub>2</sub>O<sub>3</sub> nanocomposite in simulated body fluid. *J Mater Eng Perform* 2018;27:3419–28.
- [152] Cao NQ, Pham DN, Kai N, Dinh HV, Hiromoto S, Kobayashi E. In vitro corrosion properties of Mg matrix in situ composites fabricated by spark plasma sintering. *Metals* 2017;7:358.
- [153] Deng K, Wang C, Wang X, Wu K, Zheng M. Microstructure and elevated tensile properties of submicron SiCp/AZ91 magnesium matrix composite. *Mater Des* 2012;38:110–4.
- [154] Zhong XL, Wong WLE, Gupta M. Enhancing strength and ductility of magnesium by integrating it with aluminum nanoparticles. *Acta Mater* 2007;55:6338–44.
- [155] Habibnejad-Korayem M, Mahmudi R, Poole WJ. Enhanced properties of Mg-based nano-composites reinforced with Al<sub>2</sub>O<sub>3</sub> nano-particles. *Mater Sci Eng* 2009;519:198–203.
- [156] Xiao P, Gao Y, Xu F, Yang S, Li B, Li Y, et al. An investigation on grain refinement mechanism of TiB<sub>2</sub> particulate reinforced AZ91 composites and its effect on mechanical properties. *J Alloys Compd* 2019;780:237–44.
- [157] Nie KB, Wang XJ, Hu XS, Xu L, Wu K, Zheng MY. Microstructure and mechanical properties of SiC nanoparticles reinforced magnesium matrix composites fabricated by ultrasonic vibration. *Mater Sci Eng* 2011;528:5278–82.
- [158] Xiuqing Z, Haowei W, Lihua L, Xinying T, Naiheng M. The mechanical properties of magnesium matrix composites reinforced with (TiB<sub>2</sub>+TiC) ceramic particulates. *Mater Lett* 2005;59:2105–9.
- [159] Nie KB, Wang XJ, Wu K, Xu L, Zheng MY, Hu XS. Processing, microstructure and mechanical properties of magnesium matrix nanocomposites fabricated by semisolid stirring assisted ultrasonic vibration. *J Alloys Compd* 2011;509:8664–9.
- [160] Shen MJ, Ying WF, Wang XJ, Zhang MF, Wu K. Development of high performance magnesium matrix nanocomposites using nano-SiC particulates as reinforcement. *J Mater Eng Perform* 2015;24:3798–807.
- [161] Khanra AK, Jung HC, Hong KS, Shin KS. Comparative property study on extruded Mg–HAP and ZM61–HAP composites. *Mater Sci Eng* 2010;527:6283–8.
- [162] Cao G, Konishi H, Li X. Mechanical properties and microstructure of Mg/SiC nanocomposites fabricated by ultrasonic cavitation based nanomanufacturing. *J Manuf Sci Eng* 2008;130:031105.
- [163] Meenashisundaram GK, Nai MH, Gupta M. Effects of Ti and TiB<sub>2</sub> nanoparticulates on room temperature mechanical properties and in vitro degradation of pure Mg. In: *Magnes. Technol.* Springer; 2015. p. 413–8.
- [164] Chiu C, Liu H-C. Mechanical properties and corrosion behavior of WZ73 Mg alloy/SiCp composite fabricated by stir casting method. *Metals* 2018;8:424.
- [165] Wan Y, Cui T, Li W, Li C, Xiao J, Zhu Y, et al. Mechanical and biological properties of bioglass/magnesium composites prepared via microwave sintering route. *Mater Des* 2016;99:521–7.
- [166] Güler Ö, Bağcı N. A short review on mechanical properties of graphene reinforced metal matrix composites. *J. Mater. Res. Technol.* 2020;9:6808–33.
- [167] Zhang Z, Chen DL. Consideration of Orowan strengthening effect in particulate-reinforced metal matrix nanocomposites: a model for predicting their yield strength. *Scripta Mater* 2006;54:1321–6.
- [168] Shen MJ, Wang XJ, Ying T, Wu K, Song WJ. Characteristics and mechanical properties of magnesium matrix composites reinforced with micron/submicron/nano SiC particles. *J Alloys Compd* 2016;686:831–40.
- [169] Deng K, Shi J, Wang C, Wang X, Wu Y, Nie K, et al. Microstructure and strengthening mechanism of bimodal size particle reinforced magnesium matrix composite. *Compos Part A Appl Sci Manuf* 2012;43:1280–4.
- [170] Zhou S, Deng K, Li J, Shang S, Liang W, Fan J. Effects of volume ratio on the microstructure and mechanical properties of particle reinforced magnesium matrix composite. *Mater Des* 2014;63:672–7.
- [171] Shahin M, Munir K, Wen C, Li Y. Magnesium-based composites reinforced with graphene nanoplatelets as biodegradable implant materials. *J Alloys Compd* 2020;828:154461.
- [172] Garcés G, Rodríguez M, Perez P, Adeva P. Effect of volume fraction and particle size on the microstructure and plastic deformation of Mg–Y<sub>2</sub>O<sub>3</sub> composites. *Mater Sci Eng* 2006;419:357–64.
- [173] Zhang Y, Topping T, Li Y, Vogt R, Zhou Y, Haines C, et al. Mechanical behavior of ultrafine-grained Al composites reinforced with B4C nanoparticles. *Scripta Mater* 2011;65:652–5.

- [174] Zan YN, Zhou YT, Liu ZY, Ma GN, Wang D, Wang QZ, et al. Enhancing strength and ductility synergy through heterogeneous structure design in nanoscale  $\text{Al}_2\text{O}_3$  particulate reinforced Al composites. *Mater Des* 2019;166:107629.
- [175] Sankaranarayanan S, Jayalakshmi S, Gupta M. Enhancing the ductility of Mg-(5.6 Ti+ 3Al) composite using nano-B4C addition and heat treatment. *SOJ Mater. Sci. Eng.* 2013;1:3.
- [176] Rashad M, Pan F, Lin D, Asif M. High temperature mechanical behavior of AZ61 magnesium alloy reinforced with graphene nanoplatelets. *Mater Des* 2016;89:1242–50.
- [177] Hassan SF, Paramsothy M, Gasem ZM, Patel F, Gupta M. Effect of carbon nanotube on high-temperature formability of AZ31 magnesium alloy. *J Mater Eng Perform* 2014;23:2984–91.
- [178] Dai LH, Ling Z, Bai YL. Size-dependent inelastic behavior of particle-reinforced metal–matrix composites. *Compos Sci Technol* 2001;61:1057–63.
- [179] Li Z, Gu X, Lou S, Zheng Y. The development of binary Mg–Ca alloys for use as biodegradable materials within bone. *Biomaterials* 2008;29:1329–44.
- [180] Esmaily M, Svensson JE, Fajardo S, Birbilis N, Frankel GS, Virtanen S, et al. Fundamentals and advances in magnesium alloy corrosion. *Prog Mater Sci* 2017;89:92–193.
- [181] Yang L, Zhang E. Biocorrosion behavior of magnesium alloy in different simulated fluids for biomedical application. *Mater Sci Eng C* 2009;29:1691–6.
- [182] Zhen Z, Xi T, Zheng Y. A review on in vitro corrosion performance test of biodegradable metallic materials. *Trans Nonferrous Metals Soc China* 2013;23:2283–93.
- [183] Gu X, Zhou W, Zheng Y, Dong L, Xi Y, Chai D. Microstructure, mechanical property, bio-corrosion and cytotoxicity evaluations of Mg/HA composites. *Mater Sci Eng C* 2010;30:827–32.
- [184] Li Z. Mg/Hydroxyapatite composites for potential biomedical applications. 2010.
- [185] Zheng YF, Gu XN, Xi YL, Chai DL. In vitro degradation and cytotoxicity of Mg/Ca composites produced by powder metallurgy. *Acta Biomater* 2010;6:1783–91.
- [186] Su Y, Li D, Su Y, Lu C, Niu L, Lian J, et al. Improvement of the biodegradation property and biomineralization ability of magnesium–hydroxyapatite composites with dicalcium phosphate dihydrate and hydroxyapatite coatings. *ACS Biomater Sci Eng* 2016;2:818–28.
- [187] Yin Yee Chin P, Cheok Q, Glowacz A, Caesarendra W. A review of in-vivo and in-vitro real-time corrosion monitoring systems of biodegradable metal implants. *Appl Sci* 2020;10:3141.
- [188] Hofstetter J, Martinelli E, Weinberg AM, Becker M, Mingler B, Uggowitz PJ, et al. Assessing the degradation performance of ultrahigh-purity magnesium in vitro and in vivo. *Corrosion Sci* 2015;91:29–36.
- [189] Ye X, Chen M, Yang M, Wei J, Liu D. In vitro corrosion resistance and cytocompatibility of nano-hydroxyapatite reinforced Mg–Zn–Zr composites. *J Mater Sci Mater Med* 2010;21:1321–8.
- [190] Bakhsheshi-Rad HR, Hamzah E, Staiger MP, Dias GJ, Hadisi Z, Saheban M, et al. Drug release, cytocompatibility, bioactivity, and antibacterial activity of doxycycline loaded Mg–Ca– $\text{TiO}_2$  composite scaffold. *Mater Des* 2018;139:212–21.
- [191] Sezer N, Evis Z, Koç M. Additive manufacturing of biodegradable magnesium implants and scaffolds: review of the recent advances and research trends. *J Magnes Alloy* 2021;9:392–415.
- [192] Yuan L, Ding S, Wen C. Additive manufacturing technology for porous metal implant applications and triple minimal surface structures: a review. *Bioact. Mater.* 2019;4:56–70.
- [193] Lespinasse VD, Fisher GC, Eisenstaedt J. A practical mechanical method of end-to-end anastomosis of blood-vessels: using absorbable magnesium rings. *J Am Med Assoc* 1910;55:1785–90.
- [194] Lin W, Qin L, Qi H, Zhang D, Zhang G, Gao R, et al. Long-term in vivo corrosion behavior, biocompatibility and bioresorption mechanism of a bioresorbable nitrided iron scaffold. *Acta Biomater* 2017;54:454–68.
- [195] Ulum MF, Caesarendra W, Alavi R, Hermawan H. In-Vivo corrosion characterization and assessment of absorbable metal implants. *Coatings* 2019;9:282.
- [196] Sanchez AHM, Luthringer BJC, Feyerabend F, Willumeit R. Mg and Mg alloys: how comparable are in vitro and in vivo corrosion rates? A review. *Acta Biomater* 2015;13:16–31.
- [197] Mei D, Lamaka SV, Lu X, Zheludkevich ML. Selecting medium for corrosion testing of bioabsorbable magnesium and other metals—a critical review. *Corrosion Sci* 2020;15:108722.
- [198] Falcon LA, Bedolla B E, Lemus J, Leon C, Rosales I, Gonzalez-Rodriguez JG. Corrosion behavior of Mg–Al/TiC composites in NaCl solution. *Int. J. Corros.* 2011;2011.
- [199] Agarwal S, Curtin J, Duffy B, Jaiswal S. Biodegradable magnesium alloys for orthopaedic applications: a review on corrosion, biocompatibility and surface modifications. *Mater Sci Eng C* 2016;68:948–63.
- [200] Witte F, Ulrich H, Rudert M, Willbold E. Biodegradable magnesium scaffolds: Part 1: appropriate inflammatory response. *J Biomed Mater Res* 2007;81:748–56.
- [201] Gu X, Zheng Y, Cheng Y, Zhong S, Xi T. In vitro corrosion and biocompatibility of binary magnesium alloys. *Biomaterials* 2009;30:484–98.
- [202] ISO 10993-5 biological evaluation of medical devices Part 5:tests for in vitro cytotoxicity. Switz. *Int. Organ. Stand.* 1999.
- [203] ISO 10993-12 biological evaluation of medical devices Part 12: sample preparation and reference materials. Switz. *Int. Organ. Stand.* 2007.
- [204] Witte F, Hort N, Vogt C, Cohen S, Kainer KU, Willumeit R, et al. Degradable biomaterials based on magnesium corrosion. *Curr Opin Solid State Mater Sci* 2008;12:63–72.
- [205] Huan ZG, Leeftang MA, Zhou J, Fratila-Apachitei LE, Duszczek J. In vitro degradation behavior and cytocompatibility of Mg–Zn–Zr alloys. *J Mater Sci Mater Med* 2010;21:2623–35.
- [206] Wong CWR. Biocompatibility of metal matrix composites used for biomedical applications. 2021.
- [207] Eivani AR, Tabatabaei F, Khavandi AR, Tajabadi M, Mehdizade M, Jafarian HR, et al. The effect of addition of hardystonite on the strength, ductility and corrosion resistance of WE43 magnesium alloy. *J. Mater. Res. Technol.* 2021;13:1855–65.
- [208] Li J, Ren X, Zhang Y, Hou H. Silicon carbide sintered by magnesium additive: role of pores. *J Mater Res Technol* 2020;9:6957–61.
- [209] Liu F, Li Y, Sun Z, Ji Y. Corrosion resistance and tribological behavior of particles reinforced AZ31 magnesium matrix composites developed by friction stir processing. *J Mater Res Technol* 2021;11:1019–30.

- [210] Liu D, Yang D, Li X, Hu S. Mechanical properties, corrosion resistance and biocompatibilities of degradable Mg-RE alloys: a review. *J Mater Res Technol*. 2019;8:1538–49.
- [211] Chen S, Guan S, Li W, Wang H, Chen J, Wang Y, et al. In vivo degradation and bone response of a composite coating on Mg–Zn–Ca alloy prepared by microarc oxidation and electrochemical deposition. *J Biomed Mater Res B Appl Biomater* 2012;100:533–43.
- [212] Zhou X, OuYang J, Li L, Liu Q, Liu C, Tang M, et al. In vitro and in vivo anti-corrosion properties and bio-compatibility of 5β-TCP/Mg-3Zn scaffold coated with dopamine-gelatin composite. *Surf Coating Technol* 2019;374:152–63.
- [213] Yu K, Chen L, Zhao J, Wang R, Dai Y, Huang Q. In vivo biocompatibility and biodegradation of a Mg-15% Ca<sub>3</sub>(PO<sub>4</sub>)<sub>2</sub> composite as an implant material. *Mater Lett* 2013;98:22–5.
- [214] Mahmoud A, Ezgi Ö, Merve A, Özhan G. In vitro toxicological assessment of magnesium oxide nanoparticle exposure in several mammalian cell types. *Int J Toxicol* 2016;35:429–37.
- [215] Zhao D, Huang S, Lu F, Wang B, Yang L, Qin L, et al. Vascularized bone grafting fixed by biodegradable magnesium screw for treating osteonecrosis of the femoral head. *Biomaterials* 2016;81:84–92.
- [216] Gu XN, Xie XH, Li N, Zheng YF, Qin L. In vitro and in vivo studies on a Mg–Sr binary alloy system developed as a new kind of biodegradable metal. *Acta Biomater* 2012;8:2360–74.
- [217] Saberi A, Bakhsheshi-Rad HR, Karamian E, Kasiri-Asgarani M, Ghomi H. Magnesium-graphene nano-platelet composites: corrosion behavior, mechanical and biological properties. *J Alloys Compd* 2020;821:153379.
- [218] Jabbarzare S, Bakhsheshi-Rad HR, Nourbakh A, Ahmadi T, Berto F. Effect of graphene-oxide on corrosion, mechanical and biological properties of Mg-based nanocomposite. *Int J Mineral Metallurg Mater* 2020. <https://doi.org/10.1007/s12613-020-2201-2>.
- [219] Razzaghi M, Kasiri-Asgarani M, Bakhsheshi-Rad HR, Ghayour H. In vitro degradation, antibacterial activity and cytotoxicity of Mg-3Zn-xAg nanocomposites synthesized by mechanical alloying for implant applications. *J Mater Eng Perform* 2019;28:1441–55.
- [220] Saheban M, Bakhsheshi-Rad HR, Kasiri-Asgarani M, Hamzah E, Ismail AF, Aziz M, et al. Effect of zeolite on the corrosion behavior, biocompatibility and antibacterial activity of porous magnesium/zeolite composite scaffolds. *Mater Technol* 2019;34:258–69.
- [221] Khalajabadi SZ, Kadir MR, Izman S, Bakhsheshi-Rad HR, Farahany S. Effect of mechanical alloying on the phase evolution, microstructure and bio-corrosion properties of a Mg/HA/TiO<sub>2</sub>/MgO nanocomposite. *Ceram Int* 2014;40:16743–59.
- [222] Razzaghi M, Kasiri-Asgarani M, Bakhsheshi-Rad HR, Ghayour H. Microstructure, mechanical properties, and in-vitro biocompatibility of nano-NiTi reinforced Mg–3Zn-0.5 Ag alloy: prepared by mechanical alloying for implant applications. *Compos B Eng* 2020;190:107947.



**F. Khorashadizad** earned her MSc degree in Department of Materials and Metallurgical Engineering, Iran University of Science and Technology. Her research interests include biomaterials, and nanobiomaterials.



**S. Abazari** earned her MSc degree in Department of Materials and Metallurgical Engineering, Iran University of Science and Technology. She is currently a PhD student in biomedical engineering at Amirkabir University on Technology (Tehran Polytechnic), Iran. Her research interests include biomaterials, biodegradable magnesium-based composite and nanobiomaterials.



**M. Rajabi** earned his MSc degree in Department of Materials and Metallurgical Engineering, Iran University of Science and Technology. His research interests include biomaterials, and nanobiomaterials.



**Hamid Reza Bakhsheshi-Rad** earned his PhD in materials engineering from Universiti Teknologi Malaysia (UTM) in 2013. He is an assistant professor in the Department of Materials Engineering at Najafabad Branch, Islamic Azad University, Iran. His research interests include new biodegradable magnesium, iron, zinc and their alloys and scaffolds for biomedical applications, surface modification, nanostructured metals and ceramics, polymers and composites. [https://scholar.google.com/citations?hl=en&user=PFZA\\_BoAAAAJ](https://scholar.google.com/citations?hl=en&user=PFZA_BoAAAAJ)



**Ahmad Fauzi Ismail** is a professor at the School of Chemical and Energy Engineering, Faculty of Engineering, Universiti Teknologi Malaysia (UTM). His research interest are in development of polymeric, inorganic and novel mixed-matrix membranes for water desalination, waste water treatment, gas separation processes, membranes for palm oil refining, photocatalytic membranes for removal of emerging contaminants, development of haemodialysis membranes and polymer electrolyte membranes for fuel cell applications. He is the author of over 900 papers in refereed journals and over 60 book chapters. He has authored or co-authored six books and edited or co-edited 11 books, nine patents granted and 21 patents pending. His current Scopus h-index is 78 (Citation 28 386) and Web of Science h-index is 74 (Citation 25 374). Professor Fauzi has more than 27 years integrated combination experience in the academic and research environment. He is involved extensively in R&D&C for national and multinational companies related to membrane-based processes for industrial application and currently has two spin-off companies. He is the founder of the Advanced Membrane Technology Research Center (AMTEC) and now recognized as Higher Education Centre of Excellence (HICoE). Currently he is the Distinguished Fellow at AMTEC and Deputy Vice Chancellor (Research & Innovation), UTM. <https://scholar.google.com/citations?hl=en&user=x1cug7AAAAAJ>





**Safian Sharif** is a professor in the Faculty of Engineering, Universiti Teknologi Malaysia (UTM). His research interest is in development of biodegradable magnesium, iron, zinc and their alloys and nanocomposite and 3D printing for biomedical and industrial applications. <https://scholar.google.com/citations?hl=en&user=tQ-aNkQAAAAJ>



**Seeram Ramakrishna**, FEng, Everest Chair, is among the top three impactful authors at the National University of Singapore (<https://academic.microsoft.com/institution/165932596>). Thomson Reuters identified him among the World's Most Influential Scientific Minds. Google Scholar lists him among the top 10 researchers in materials science ([https://scholar.google.com.sg/citations?view\\_op=search\\_authors&hl=en&mauthors=label:materials\\_science](https://scholar.google.com.sg/citations?view_op=search_authors&hl=en&mauthors=label:materials_science)).

Clarivate Analytics recognized him among the Top 1% Highly Cited Researchers in the world. Microsoft Academic ranked him among the top 50 impactful persons out of 3 million materials researchers worldwide (<https://academic.microsoft.com/authors/192562407>). <https://scholar.google.com/citations?hl=en&user=a49NVmkAAAAJ>.



**Filippo Berto** earned his degree summa cum laude in industrial engineering in 2003 at the University of Padua (Italy). After attending the PhD course in mechanical engineering and materials science at the University of Florence, he worked as a researcher in the same field at the University of Padua. From 2006 to 2013 he was Assistant Professor at the University of Padua, Department of Management and Engineering, Vicenza and from October 2014 to September 2016 he was Associate Professor. In January 2016 he was appointed as international outstanding renowned Chair of Fracture Mechanics and Fatigue. <https://scholar.google.com/citations?hl=en&user=HgYct2UAAAAJ>